

2019

# The effect of dissolved nickel and copper on the adult coral *Acropora muricata* and its microbiome

Francesca Gissi

*CSIRO Oceans and Atmosphere, University of Wollongong, fg409@uowmail.edu.au*

Amanda Reichelt-Brushett

*Southern Cross University*

Anthony A. Chariton

*Macquarie University, Anthony.Chariton@csiro.au*

Jenny Stauber

*CSIRO Land and Water, jenny.stauber@csiro.au*

Paul Greenfield

*Macquarie University, CSIRO Energy*

*See next page for additional authors*

---

## Publication Details

Gissi, F., Reichelt-Brushett, A. J., Chariton, A. A., Stauber, J. L., Greenfield, P., Humphrey, C., Salmon, M., Stephenson, S. A., Cresswell, T. & Jolley, D. F. (2019). The effect of dissolved nickel and copper on the adult coral *Acropora muricata* and its microbiome. *Environmental Pollution*, 250 792-806.

---

# The effect of dissolved nickel and copper on the adult coral *Acropora muricata* and its microbiome

## Abstract

The potential impacts of mining activities on tropical coastal ecosystems are poorly understood. In particular, limited information is available on the effects of metals on scleractinian corals which are foundation species that form vital structural habitats supporting other biota. This study investigated the effects of dissolved nickel and copper on the coral *Acropora muricata* and its associated microbiota. Corals collected from the Great Barrier Reef were exposed to dissolved nickel (45, 90, 470, 900 and 9050 µg Ni/L) or copper (4, 11, 32 and 65 µg Cu/L) in flow through chambers at the National Sea Simulator, Townsville, Qld, Australia. After a 96-h exposure DNA metabarcoding (16S rDNA and 18S rDNA) was undertaken on all samples to detect changes in the structure of the coral microbiome. The controls remained healthy throughout the study period. After 36 h, bleaching was only observed in corals exposed to 32 and 65 µg Cu/L and very high nickel concentrations (9050 µg Ni/L). At 96 h, significant discolouration of corals was only observed in 470 and 900 µg Ni/L treatments, the highest concentrations tested. While high concentrations of nickel caused bleaching, no changes in the composition of their microbiome communities were observed. In contrast, exposure to copper not only resulted in bleaching, but altered the composition of both the eukaryote and bacterial communities of the coral's microbiomes. Our findings showed that these effects were only evident at relatively high concentrations of nickel and copper, reflecting concentrations observed only in extremely polluted environments. Elevated metal concentrations have the capacity to alter the microbiomes which are inherently linked to coral health.

## Keywords

dissolved, nickel, copper, effect, adult, its, microbiome, acropora, muricata, coral

## Publication Details

Gissi, F., Reichelt-Brushett, A. J., Chariton, A. A., Stauber, J. L., Greenfield, P., Humphrey, C., Salmon, M., Stephenson, S. A., Cresswell, T. & Jolley, D. F. (2019). The effect of dissolved nickel and copper on the adult coral *Acropora muricata* and its microbiome. *Environmental Pollution*, 250 792-806.

## Authors

Francesca Gissi, Amanda Reichelt-Brushett, Anthony A. Chariton, Jenny Stauber, Paul Greenfield, Craig Humphrey, Matt Salmon, Sarah Stephenson, Tom Cresswell, and Dianne F. Jolley

## **The effect of dissolved nickel and copper on the adult coral *Acropora muricata* and its microbiome**

Francesca Gissi<sup>1,2\*</sup>, Amanda Reichelt-Brushett<sup>3</sup>, Anthony Chariton<sup>4</sup>, Jenny Stauber<sup>5</sup>, Paul Greenfield<sup>4,6</sup>, Craig Humphrey<sup>7</sup>, Matt Salmon<sup>7</sup>, Sarah Stephenson<sup>1</sup>, Tom Cresswell<sup>8</sup>, and Dianne Jolley<sup>2</sup>

<sup>1</sup> CSIRO Oceans and Atmosphere, Locked Bag 2007 Kirrawee, NSW, 2232, Australia.

<sup>2</sup> School of Chemistry, University of Wollongong, NSW, Australia

<sup>3</sup> School of Environment, Science and Engineering, Southern Cross University, Lismore, NSW Australia.

<sup>4</sup> Department of Biological Sciences, Macquarie University, NSW Australia.

<sup>5</sup> CSIRO Land and Water, NSW Australia.

<sup>6</sup> CSIRO Energy, North Ryde, NSW, Australia.

<sup>7</sup> National Sea Simulator, Australian Institute of Marine Science, Townsville, QLD

<sup>8</sup> ANSTO, 2232, NSW, Australia.

\*Corresponding author:

Francesca Gissi

Email: [Francesca.gissi@csiro.au](mailto:Francesca.gissi@csiro.au)

Current address: Environmental Forensics, Science Division, Office of Environment and Heritage, NSW Australia.

## Abstract

The potential impacts of mining activities on tropical coastal ecosystems are poorly understood. In particular, limited information is available on the effects of metals on scleractinian corals which are foundation species that form vital structural habitats supporting other biota. This study investigated the effects of dissolved nickel and copper on the coral *Acropora muricata* and its associated microbiota. Corals collected from the Great Barrier Reef were exposed to dissolved nickel (45, 90, 470, 900 and 9050 µg Ni/L) or copper (4, 11, 32 and 65 µg Cu/L) in flow through chambers at the National Sea Simulator, Townsville, Qld, Australia. After a 96-h exposure DNA metabarcoding (16S rDNA and 18S rDNA) was undertaken on all samples to detect changes in the structure of the coral microbiome. The controls remained healthy throughout the study period. After 36 h, bleaching was only observed in corals exposed to 32 and 65 µg Cu/L and very high nickel concentrations (9050 µg Ni/L). At 96 h, significant discolouration of corals was only observed in 470 and 900 µg Ni/L treatments, the highest concentrations tested. While high concentrations of nickel caused bleaching, no changes in the composition of their microbiome communities were observed. In contrast, exposure to copper not only resulted in bleaching, but altered the composition of both the eukaryote and bacterial communities of the coral's microbiomes. Our findings showed that these effects were only evident at relatively high concentrations of nickel and copper, reflecting concentrations observed only in extremely polluted environments. Elevated metal concentrations have the capacity to alter the microbiomes which are inherently linked to coral health.

**Capsule:** Bleaching and changes in the coral microbiome community structure were only observed in corals exposed to high concentrations of dissolved nickel and copper.

**Keywords:** Coral microbiome, 16S rDNA, 18S rDNA , Tropical ecotoxicology, DNA metabarcoding, Metals

## Highlights

- There is an increase in mining activities in tropical regions
- Corals may be exposed to metal contaminants
- There is limited data for the effects of metals on adult corals and their microbiome
- We exposed the coral *Acropora muricata* to Cu and Ni separately

- High concentrations of Cu and Ni caused bleaching and changes in the microbiome community of *A. muricata*

## 1. Introduction

Mining and production of metals has recently intensified in the Asia-Pacific region (USGS, 2016). However, there has been limited research on the potential impacts of these activities in the tropical coastal marine environment, hindering the establishment of ecologically-relevant risk assessment tools, e.g. water quality guideline values. Temperate marine water guideline values for copper and nickel have been developed in various jurisdictions e.g. 1.3 µg Cu/L and 7 µg Ni/L, respectively (ANZECC/ARMCANZ, 2000). Such guideline values are yet to be developed for tropical environments due to a paucity of relevant data for endemic species (Gissi et al., 2016). Corals are foundational species in tropical marine systems, thus understanding the impacts of metal contaminants on corals is pivotal for developing ecologically relevant risk assessment and management strategies for mining operations in tropical marine environments.

Coral reefs are increasingly exposed to a variety of anthropogenic stressors. While the effects of climate change (e.g. increase in temperature and decrease in pH) and agricultural run-off (i.e. increasing loadings of pesticides and nutrients) are well documented (Bessell-Browne et al., 2017; Biscere et al., 2015; Flores et al., 2012; Negri et al., 2011; Nystrom et al., 2001), in some environments, metals may also be contributing to the decline in the health of coral ecosystems (Mitchelmore et al., 2007). Exposure to elevated metals has been shown to elicit a range of ecotoxicological effects on corals across all life stages: including coral fertilisation (e.g. Reichelt-Brushett and Harrison, 2005); larvae survival and motility (Reichelt-Brushett and Harrison, 2004); settlement and metamorphosis of larvae (Negri and Heyward, 2001; Reichelt-Brushett and Harrison, 2000); and bleaching (expulsion of *Symbiodinium*) and photosynthetic efficiency in adult corals (Jones, 1997). Copper is generally more toxic than nickel to all coral life stages; however, there are far fewer studies which have investigated nickel toxicity to corals. Copper inhibits coral fertilisation, larval metamorphosis and survival between 15 – 150 µg Cu/L, as cited in Gissi et al., (2017). Survival of adult corals has been shown to be reduced by 50% at 250 µg Cu/L (Hedouin et al., 2016). Nickel has been found to inhibit fertilisation success but only at very high concentrations, >1000 µg Ni/L (Gissi et al., 2017; Reichelt-Brushett and Hudspith, 2016; Reichelt-Brushett and Harrison, 2005) and to inhibit larval survival and settlement at 9000 µg Ni/L (Goh, 1991). To date, there are few reports on the toxicity of nickel to adult corals (Biscéré et al., 2017).

The coral microbiome consists of bacteria, dinoflagellate algae of the genus *Symbiodinium*, viruses, fungi and archaea (Peixoto et al., 2017). The microbiome plays a fundamental role in the development, health and defence of the coral host (Hernandez-Agreda et al., 2017). Microbial communities contribute to carbon and sulfur cycling, phosphorous fixation, metal homeostasis, organic remediation, production of antibiotics and secondary metabolism (reviewed by McDevitt-Irwin et al., 2017). To gain a better understanding of the effects of contaminant exposure on the host, it is pivotal that corals and their microbiota are examined collectively as 'holobionts' (McDevitt-Irwin et al., 2017). Studies on the impacts of climate change drivers have found that environmental stressors can alter the microbiome community structure, potentially reducing the health and survival of corals (Grottoli et al., 2018; Thurber et al., 2009a; Webster et al., 2016). A number of field studies have shown that the coral microbiome is also susceptible to anthropogenic impacts from sedimentation, sewage and municipal waste water discharge and changes in salinity (Paulino et al., 2016; Rothig et al., 2016; Zhang et al., 2015; Ziegler et al., 2016).

To our knowledge, there have been no studies which have investigated the effects of individual metals on the entire coral holobiont (coral animal host, bacteria and algal endosymbionts). Bielmyer et al. (2010) showed that the response of staghorn corals and their algal endosymbionts to copper varied. In the coral *Acropora cervicornis*, copper had accumulated in the associated *Symbiodinium* and photosynthesis was also affected. Photosynthesis was also adversely affected in *Symbiodinium* of *Pocillopora damicornis*, although copper accumulation was not detected in either animal or algal tissue (Bielmyer et al., 2010). One study has shown that in the microbiome of tropical marine sponges the bacterial diversity was reduced by 64% following 48-h exposure to 223 µg Cu/L (Webster et al., 2001). Microbes are key in the functioning and stability of coral reefs, and respond rapidly to environmental change, including declining water quality. Therefore microbes could potentially be used as early warning indicators for environmental stress and coral reef health, rather than traditional monitoring methods based on visual signs of health deterioration (e.g. bleaching) (Glasl et al., 2017). However, there are still significant knowledge gaps concerning the roles of the microbiome and cnidarian host during stress, particularly when exposed to metals.

The aim of this study was to investigate how increasing concentrations of dissolved copper and nickel, individually, affect the condition of adult corals and their associated microbiomes. We

hypothesised that increasing concentrations of metals would alter the structure of the coral microbiome, and this could potentially reduce the adaptive ability of corals to deal with stress. Metal concentrations were chosen based on the few studies available in the literature. The concentration ranges for both copper and nickel were high, above environmentally relevant concentrations in order to capture the full concentration-response relationship as previous studies have shown that corals are often less sensitive to metals, such as nickel, compared to other marine invertebrates (Gissi et al., 2018). The widespread staghorn coral *Acropora muricata* was exposed separately to increasing concentrations of copper and nickel, and after 4 days the following endpoints were measured: bleaching (loss of *Symbiodinium*), accumulation and distribution of metals in corals and changes in the coral microbiome (using DNA metabarcoding).

## **2. Methods**

### *2.1. General laboratory techniques and reagents*

All glassware and plastic containers used in the tests were acid-washed in 10% (v/v) nitric acid (Reagent grade Merck) and thoroughly rinsed with demineralised water (five rinses), followed by high purity water (five rinses, Milli-Q®, 18.2 MΩ/cm; Merck). Following acid-washing, treatment tanks, tubing and test chambers were soaked in natural seawater (filtered) for at least 24 h.

All metal stock solutions were made volumetrically using high purity water. Copper stock solution of 0.1 g Cu/L was prepared using copper (II) sulfate salt (A.R. grade, AJAX Chemicals, Australia). Nickel stock solution of 1 g Ni/L was made using nickel (II) chloride hexahydrate salt (A.R. grade, Chem Supply, Australia). All stocks were acidified to 0.01% HCl (Merck, Tracepur).

Physico-chemical parameters (pH, dissolved oxygen (DO), conductivity and salinity) were measured in the treatment tanks and one randomly selected replicate chamber every day during the exposure. Parameters were measured using a Multi probe (HQ40d Multi-Hach), calibrated following instructions from the manufacturer.

### *2.2. Species collection and maintenance*

This toxicity study was carried out at the National Sea Simulator (SeaSim), Australian Institute of Marine Science (AIMS), Townsville, Australia. The scleractinian branching coral, *A. muricata*, was collected by SeaSim on the 7 June 2016 from Trunk Reef (18° 18.173'S, 146° 52.153'E), at 3 – 5 m depth, Great Barrier Reef, Queensland, Australia (GBRMPA Permit number G12/35236.1). One



colony of *A. muricata* was separated into 5-8 cm fragments on board the boat and mounted onto aragonite plugs, using super glue (XTRA Loctite super glue, Loctite Australia Pty Ltd). Coral fragments were maintained in 60-L aquaria with flowing seawater (5 L/min) from the collection point until returned to the SeaSim aquaria on the following day. Once in the SeaSim, coral fragments were maintained in natural filtered (0.04  $\mu\text{m}$ ) seawater, with day:night cycles, set to mimic conditions on the reef (2 h ramp up, 8 h at 100 – 150  $\mu\text{mol m}^{-2} \text{s}^{-1}$ , 2 h ramp down). Corals were fed a combination of newly hatched *Artemia nauplii* and microalgae (mixture of *T.Isochrysis lutea*, *Pavlova lutheri*, *Dunaliella* sp, *Nannochloropsis oceania*, *Chaetoceros muelleri*, and *Chaetoceros calcitrans* at  $5 \times 10^6$  cells/mL).

### 2.3. Toxicity testing with adult corals

Toxicity tests commenced on the 15 July 2016, approximately 5 weeks after acclimation to aquaria conditions. There is no established protocol for acclimating adult corals prior to testing in aquaria conditions; however, the health of the corals was noted by observing the colour of the fragments and the presence of skeletal growth around the base of the fragments on the aragonite plugs.

Treatment solutions were made in 80-L acrylic tanks by diluting metal stock solutions in natural filtered (0.04  $\mu\text{m}$ ) seawater. Filtered seawater is stored in a covered dam before delivery to experimental systems. On day 0, 40 L of each treatment solution was prepared. To top up the tanks on subsequent days (days 1-3), 20 L of each treatment solution was made and added to the respective tanks. Treatment solutions were fed to test chambers via linear low-density polyethylene (LLDPE) tubing, using peristaltic pumps (Masterflex® L/S Digital Std drive. Extech Equipment Pty Ltd, VIC, AUS). Custom test chambers were 2.5 L, with clear acrylic lids (to allow for light penetration) and an acrylic container. Treatment solutions were delivered into the top of each chamber, with submersible magnetic stirrers to provide water movement (Figure 1). Test chambers were housed in a single water bath to allow for accurate temperature control. The total volume of treatment solution in each chamber was 2 L and the flow rate for each chamber was 2.8 mL/minute which resulted in an 80-90% water exchange, twice every 24 h. Coral fragments on aragonite plugs were inserted into the mounting plates in each chamber (Figure 1). There were four replicate chambers per treatment, with three fragments in each chamber. Full details on the toxicity test parameters are provided in Table 1.

Table 1. Toxicity test conditions and parameters for 96-h exposure with *Acropora muricata*

<b>Test conditions/parameters</b>	
Temperature (°C)	27 ± 0.5
Salinity (psu)	35 ± 1
DO (%)	>80
pH	8.1 ± 0.2
Nickel treatments (µg/L)	50, 100, 500, 1000, 10000
Copper treatments (µg/L)	5, 20, 50, 100
Light parameters	Low light 6:30 (dawn) Full light 8:00 (100-150 µmol/m <sup>2</sup> /s). Irradiance was similar to the expected mean photosynthetically active radiation at the collection site. Low light 16:00 (dusk) Lights off 18:00
Test type	Flow through: 2.8 mL/day/chamber, 80-90% of water exchanged 2 x per day in each chamber.
Test chamber	2.5 L acrylic container and lid, water circulation within chamber maintained with magnetic stirrer bar controlled by water pressure (Figure 1).
Test volume	2 L
Test duration	96 h
Control/diluent water	0.04 µm natural filtered seawater
Life stage of test organism	Adult, 5-8 cm fragments

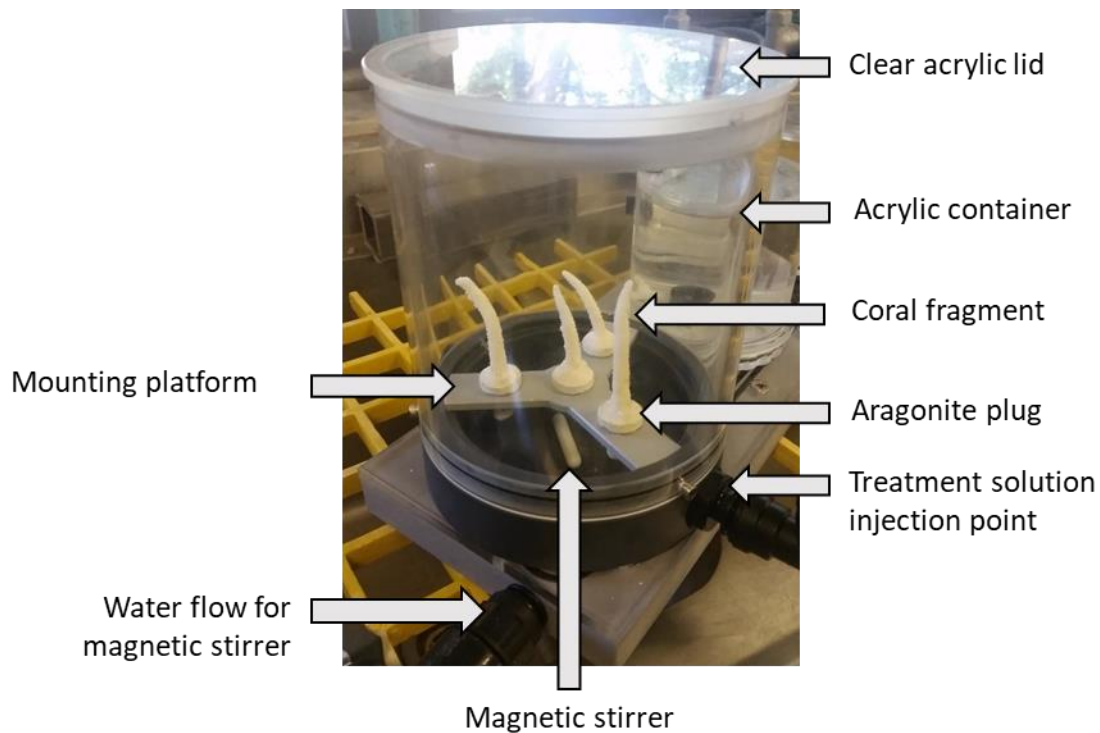


Figure 1. Design of the coral test Chamber. Note only three coral fragments were placed in each chamber, in this study.

At 36 h, severe bleaching was observed in the following treatments: 20, 50 and 100  $\mu\text{g Cu/L}$  and 10 000  $\mu\text{g Ni/L}$  (nominal values). To ensure these treatments could still be sampled for tissues, these fragments were sampled and processed (described below) at 36 h. On day 4, remaining fragments were removed from chambers, rinsed in seawater (note: fragments collected at 36 h were not rinsed in seawater due to severe tissue degradation), and photographed for assessment of bleaching. The coral watch health chart was used to assess the degree of bleaching in coral fragments following exposure (Coral Watch, 2014). The exposure duration of 96 h was chosen to allow for comparison with other marine invertebrate studies investigating the toxicity of metals and because this duration is standard in acute toxicity testing protocols (e.g. OECD, ASTM). Three fragments from each chamber were processed for the following measurements:

Fragment 1: Quantification of metals in coral tissues. The fragment was rinsed in clean seawater, placed in clean/new ziplock bag and air blasted to remove tissues which were transferred into a 5-mL polypropylene vial and acidified to 2%  $\text{HNO}_3$  (Tracepur).

Fragment 2: Spatial distribution of metals in coral fragments. The fragment was rinsed in clean seawater put in a clean/new zip lock bag, made air tight and stored in a freezer (-20°C).

Fragment 3: Changes in coral microbiome community structure – DNA metabarcoding. The fragment was rinsed in seawater, placed in clean/new ziplock bag and air blasted to remove tissues. The tissue slurry was pipetted (using sterile pipettes) into 2 mL cryo vials and flash frozen in liquid nitrogen and stored at -80°C until DNA extraction.

#### 2.4. *Quantification of metals in coral tissues*

Nickel and copper-exposed coral and *Symbiodinium* tissue (combined) samples were transferred to pre-weighed, acid washed, 50-mL digest tubes. Samples were oven dried at 60°C for 24 h and weighed to determine dry mass ( $0.08 \pm 0.03$  g) of sample to be digested. Dried tissues were combined with 5 mL of concentrated HNO<sub>3</sub> (Merck, Tracepur) and left with loosened lids in a fume hood overnight. Tubes were then heated (hot block, Digi Prep MS, SCP Science) to 60°C for 2 h (with a 30 min ramp up to the max temperature). Digested samples were allowed to cool in a fume hood, and diluted to a final concentration of 6.6% HNO<sub>3</sub> with high purity water. Samples were analysed by inductively coupled plasma-atomic emission spectroscopy (ICP-AES, section 2.6). Samples included tissues, three laboratory blanks (from the time of sampling the corals), three digestion blanks, and three certified reference material (National Institute of Standards and Technology (NIST), Standard Reference Material, SRM 2976) matching the weight range (dry weight,  $0.08 \pm 0.03$  g) of the coral samples.

#### 2.5. *Spatial distribution of nickel in coral fragments*

To investigate the distribution of nickel in the coral fragments, selected coral samples were analysed using the ITRAX X-ray fluorescence, Laser Ablation inductively coupled plasma mass spectroscopy (LA-ICPMS) and micro Particle-Induced X-ray Emission ( $\mu$ -PIXE) at ANSTO, NSW, Australia. To our knowledge, this is the first time these instruments have been used to measure nickel in whole coral samples (skeletons and tissues). For the ITRAX analysis, one control and one Ni-exposed fragment (500  $\mu$ g Ni/L) were analysed. No significant difference between the control and nickel-exposed coral fragment was detected and so this method was not pursued further (data not shown).

For the LA-ICPMS technique one control coral fragment was analysed alongside one Ni-exposed fragment from each of the following treatments, 100, 1000 and 10 000  $\mu\text{g Ni/L}$  (nominal). Prior to analysis, coral fragments were half embedded in a paraffin wax longitudinally and cut into four (11mm) sections (termed A:D) using a diamond wire (Supplementary, Figure S1). Sections B, C and D of the coral fragment exposed to 10 000  $\mu\text{g Ni/L}$  were analysed first; subsequent measurements of other coral fragments were taken from section B only. Prior to analysis, sections were polished/sanded using a 220 grit size SiC paper, by hand, to level the surface of the coral and wax, and then cleaned with high purity water and air dried (at room temperature). Samples were analysed using a Resonetics M50 193nm Excimer laser ablation system coupled to a Varian-820 –ICP MS. A rectangular laser spot ( $20 \mu\text{m} * 100 \mu\text{m}$ ) and a laser pulse frequency of 10 Hz was used. Ablation paths were cleaned by laser at a rate of  $150 \mu\text{m/s}$  prior to analysis at  $30 \mu\text{m/s}$  with helium and nitrogen flow rate of 600 and 5 ml/min, respectively, through the sample cell. Mass spectrometry was conducted with a dwell time of 20 ms. All elements were referenced to NIST SRM612 (trace elements in glass). NIST glass references are not certified for Mg, however a reference value supplied by the lolite software (77 ppm) was used (Runnalls and Coleman, 2003). Mass spectrometry data were processed with lolite. It was not possible to normalise data using  $^{43}\text{Ca}$ , as is standard practice (Limbeck et al., 2015), due to the highly porous nature of the coral samples. Therefore, data presented for nickel exposures are semi-quantitative only.

To support the LA-ICP-MS data, sections B and D of the coral exposed to 10 000  $\mu\text{g Ni/L}$  (nominal) were analysed with  $\mu\text{-PIXE}$ . The  $\mu\text{-PIXE}$  analyses were performed on the Australian National Tandem Research Accelerator heavy ion microprobe (Siegele et al., 1999) using a 3-MeV proton beam with a spot size of approximately 5-7  $\mu\text{m}$  and a beam current of 0.3 - 1.0 nA. X-ray fluorescence spectra were collected using a high-purity Ge detector with an active area of  $100 \text{mm}^2$  approximately located 33 mm from the sample. To reduce low-energy x-rays and to prevent scattered protons from entering the detector, a 112  $\mu\text{m}$  thick Mylar foil was placed in front of the detector. Samples were scanned over an area of approximately  $2 \times 2 \text{mm}$ , which is the maximum scan area for 3-MeV protons achievable with the ANSTO microprobe. The  $\mu\text{-PIXE}$  data were analysed using GeoPIXE software (Ryan, 2001; Ryan et al., 1995) and elemental maps were extracted from the data.

## 2.6. Chemical analyses

All plasticware used for metal sub-sampling of test solutions and coral tissues was acid washed (10% v/v, Tracepur; Merck) and rinsed with high purity water in a semi-clean room. Water samples were taken from the filtered seawater entering the aquaria (used to make treatment solutions) and the treatment tanks every day during the 96-h exposure. On day 0 and day 4, sub-samples were taken from all test chambers. All dissolved metal sub-samples were filtered through acid-washed syringes and 0.45 µm sterile filters (Sartorius Ministart® Syringe Filter, Germany), collected in acid-washed 10 mL polypropylene vials. For total metals, 10 mL was collected (using an acid-washed pipette tip) from tanks and chambers and dispensed into acid-washed 10 mL polypropylene vials. All samples were acidified to 2% with Tracepur nitric acid (Tracepur; Merck) and stored at 4°C in the dark until analysis. Samples were analysed using ICP-AES (730ES). Quality assurance procedures included matrix-matched calibration standards, drift standards and seawater blanks. For tissue digests, values were reported as metal concentration in µg/kg of dried weight. The concentration factor was calculated by dividing tissue metal concentration (µg/kg) by the measured, dissolved metal concentration in the treatment solutions (µg/L).

Sub-samples were taken from the seawater used to make treatment solutions and from one replicate chamber at test completion to measure dissolved organic carbon (DOC). Samples were filtered through a 0.45 µm filter and collected in a glass vial with 2 mL of concentrated H<sub>2</sub>SO<sub>4</sub>. Analysis of DOC was conducted by the National Measurement Institute (NMI), Sydney, Australia. Samples were taken on day 0 and at test completion.

### 2.7. *DNA extraction amplification and sequencing*

Samples were removed from the -80°C freezer, gently thawed and extracted using the QIAGEN® DNeasy Power Biofilm kit (QIAGEN®, Germany), according to manufacturer instructions with the following modifications; the Fast Prep®-24 (MT™) was used to lyse the samples for 45 seconds, with the speed set to 4.5; DNA was eluted in 2 x 50µL of elution buffer and allowed to rest for 1 min before the final centrifugation step. Success of extraction and DNA yield was measured on the Nanodrop spectrophotometer (Thermo Fisher Scientific, USA).

Three different sets of primers were used to target and amplify different components of the microbial community in the coral tissues. The eukaryotic community was determined using the All18SF (5'-3': TGGTGCATGGCCGTTCTTAGT) and All18SR (5'-3': CATCTAAGGGCATCACAGACC)

primers for the V7 region of the 18S rRNA gene (Hardy et al., 2010). The bacterial composition was determined with two different primer sets to identify the most appropriate primer set. The first 16S primer set was 515f (5'-3': GTGYCAGCMGCCGCGGTAA) (Baker et al., 2003; Quince et al., 2011), 806r (5'-3': GGACTACNVGGGTWTCTAAT) (Aprill et al., 2015) for the V4 region of the 16S rRNA gene (recommended by Earth Microbiome Project, EMP). The second primer set was 784f (5'-3': AGGATTAGATACCCTGGTA), 1061r (5'-3': CRRACGAGCTGACGAC) for the V5 and V6 region of the 16S rRNA gene (Andersson et al., 2008; Ziegler et al., 2016). Results showed that the overall analysis of the community composition using either the V4 primers or the V5-V6 primers were similar; and the V4 primers provided a better coverage of the bacterial community. For these reasons only results for the V4 primers are presented here; results for V5-V6 primers are provided in the supplementary information.

The conditions for the Polymerase Chain Reaction (PCR) used to amplify with each of the primer sets is described in Table S1. All amplifications used the Amplitaq Gold 360 Master Mix (MM, Applied Biosystems) and DNA-free water (Millipore®). For 18S rDNA the total PCR reaction volume was 50 µL which consisted of 25 µL of MM, 1 µL of each primer (10 µM), 20 µL of water and 3 µL of template DNA. For the 16S rDNA, PCR reactions followed methods on the Earth Microbiome Project (EMP, <http://www.earthmicrobiome.org/protocols-and-standards/16s/>) website, and the total reaction volume was 25 µL, with 10 µL of MM, 0.5 µL of each primer (10 µM), 11 µL of water and 3 µL of template DNA. In all PCR reactions, samples were amplified alongside positive controls (mussel or crocodile DNA for 18S rDNA; Enterobacter for the 16S rDNA and negative controls (DNA-free water)). Primers were barcoded for multiplexing with each sample given a unique barcode combination following the protocol of Chariton et al. (2015).

Following amplification of either 18S rDNA or 16S rDNA, 16S and 18S rDNA samples were each pooled and PCR products were purified using the QIAGEN QIAquick® PCR purification kit. Amplification and purification success was interrogated on a MultiNA gel (Shimadzu, MCE-202), following the manufacturer's instructions. Negative controls were checked for contamination in the MultiNA gel (no contamination was detected in any PCRs used for sequencing) and were not included in the pooled samples processed for sequencing.

The final pooled amplicon library concentrations were measured on a Nanodrop and sent to the Ramaciotti Centre for Genomics (University of New South Wales, AUS) for sequencing. Amplicon

libraries were prepared for sequencing using TruSeq PCR-free kit. As the base pair sizes of the amplicons were different for 18SrDNA (180bp) and 16SrDNA (350bp), the libraries were run as two separate Illumina® Miseq sequencing runs, 2x 250bp for 16S and 2x 150bp for 18S. Raw sequences are available at <https://doi.org/10.25919/5b9745a02208a>.

## 2.8. *Bioinformatics*

Sequenced data were processed using a custom pipeline (Greenfield Hybrid Amplicon Pipeline, GHAP) which is based on USEARCH tools (Edgar, 2013). The pipeline is available at <https://doi.org/10.4225/08/59f98560eba25>. GHAP demultiplexes the sequence reads to produce a pair of files for each sample. These paired reads were merged, trimmed, de-replicated, and clustered at 97% similarity to generate a set of representative OTU (Operational Taxonomic Units) sequences. USearch v10.0.240 tools (fastq\_mergepairs, fastx\_uniques and cluster\_otus) (Edgar, 2013) were used for the merging, de-replicating and clustering steps. The 16S rDNA OTU sequences were classified in two ways: first, by using the RDP Classifier (v2.12) (Cole et al., 2014) to determine a taxonomic classification for each sequence, down to the level of genus where possible; and second, by using usearch\_global to match the representative sequence from each OTU against a 16S rRNA reference set built by merging the curated sequences from the RDP 16S training set (release 16) and the RefSeq 16S rRNA set (downloaded in July 2017). The 18S rRNA representative sequences were classified by matching them (ublast) against a curated set of 18S reference sequences derived from the SILVA v123 SSU reference set (Cole et al., 2014; Quast et al., 2012). This 18S rDNA reference set was built by taking all the eukaryote sequences from the SILVA v123 SSU dataset, and removing those sequences containing bacterial or chloroplast regions, as well as those with inconsistencies in their taxonomic lineages. A full description of this curation is provided in the GHAP documentation. The pipeline then used usearch\_global to map the merged reads from each sample back onto the OTU sequences to obtain accurate read counts for each OTU/sample pairing. The classified OTUs and the counts for each sample were finally used to generate OTU tables in both text and BIOM (v1) file formats, complete with taxonomic classifications, species assignments and counts for each sample.

## 2.9. *Statistical analyses*



After processing through the bioinformatics pipeline and prior to statistical analysis, data was processed through a final filtering step. For 18S and 16S data, the highest read for the positive control OTU in samples was 60 and 167, respectively. These two values were used as the cut-off points for filtering the dataset, with 18S rDNA and 16S rDNA OTUs with maximum detection of 60 or 167 reads deleted, respectively, thereby removing potential tag-jumped sequences and low quality read. OTUs which had a match percent of <80 were also removed. The positive controls amplified in the PCR were also used for screening of successful amplification and sequencing and to check for cross contamination in the 18S and 16S libraries. The positive controls and OTUs were removed from the dataset and this final dataset was used in the statistical analysis. For the 18S rDNA data all coral OTUs were also removed to focus on the microbiota only. Supplementary Table S3 shows the total number of reads and OTUs prior to and following this filtering step.

As there was either no, or a weak correlation between number of sequence reads and organism abundance (18S rDNA  $R^2 = -0.002$ , 16S rDNA  $R^2 = 0.3$ ) the data was not rarefied (Egge et al., 2013). The 18S rDNA dataset was transformed to presence/absence prior to computation (Chariton et al., 2015). The 16S rDNA data were initially standardised by the total abundance and then square-root transformed to calculate the relative abundance of each OTU across samples.

Multivariate analysis of the microbiome data was performed using the Primer 7+ statistical package (Plymouth Marine Laboratory, UK). Ordination was performed by non-metric multidimensional scaling (nMDS) using the Bray-Curtis similarity coefficient. Statistical differences between treatments were tested by permutational multivariate analysis of variance (PERMANOVA,  $P \leq 0.05$ ), based on 999 random permutations. Primer's SIMPER function was used to identify key taxa contributing to compositional differences between treatments, using Bray-Curtis similarity, one-way design and the cut-off percentage set to 90. For the 18S rDNA and both 16S rDNA datasets, the taxonomic levels of class and family, respectively were used. Shade plots to indicate number of OTUs in each sample were also generated in Primer.

The DIVERSE function in Primer was used to determine Shannon's diversity. Differences in these univariate attributes across treatments were examined using a one-way ANOVA with Bonferroni's (all pairs) and Tukey-Kramer tests in NCSS v7 (Utah, USA).

### **3. Results**

### 3.1. Quality control

Over the 96-h exposure period physico-chemical parameters were maintained within acceptable limits (Table 1). Dissolved organic carbon (DOC) in the filtered aquaria seawater was 1.7 mg/L on day 0. In treatment chambers sacrificed at 36 h, DOC was 1.9 – 4.3 mg/L; at 96 h, DOC in remaining chambers 1.7 – 2.2 mg/L.

The background concentrations of metals in the seawater used to make treatment solutions were generally below the limit of detection (LOD, Supplemental material Table S3). The mean of the measured dissolved concentrations in the chambers on day 0 and day 4 (or at 36 h for some treatments) was used in all following analyses (Table 2). The measured, total and dissolved concentration of nickel and copper in the tanks and chambers is provided in supplementary information (Tables S4 and S5).

Table 2. Concentrations of dissolved nickel and copper, measured in the test chambers on day 0 and day 1 or day 4. Reported values are the mean and standard deviation (SD, n=4).

Treatment	Day 0		Day 1 or 4 <sup>a</sup>		Mean for day 0 and day 4
	Mean	SD	Mean	SD	
Nominal, µg/L	Measured Dissolved (<0.45 µm), µg/L				
	Nickel				
Control <sup>b</sup>	0.9	0.6	0.9	0.3	0.9
50	43	0.6	46	0.5	45
100	87	0.6	93	0.5	90
500	467	7.9	477	2.5	470
1000	873	8.0	922	3.9	900
10000 <sup>c</sup>	8912	136	9186	38	9050
	Copper				
Control	3.2	0.5	0.8	0.2	
5	5.5	0.2	2.3	0.1	4
20 <sup>c</sup>	14	0.7	9.2	0.7	11
50 <sup>c</sup>	35	1.1	29	0.4	32
100 <sup>c</sup>	68	2.1	61	2.2	65

<sup>a</sup> For corals that were removed at 36 h, metals were sub-sampled and for these treatments the mean dissolved concentration sampled on day 1 was used. For all other treatments where the exposure ran for 96 h, the mean dissolved concentration sampled on day 4 was used.

<sup>b</sup> Where concentrations were below the limit of detection (LOD), values were supplemented with half LOD

<sup>c</sup> Corals in these treatments were sacrificed and samples taken for analysis at 36 h (not on day 4), due to bleaching.

### 3.2. Response of coral to exposure to Ni and Cu

We observed full colour, no bleaching and extended tentacles in the control (unexposed) coral fragments, indicating 100% healthy coral following 96-h exposure (Figure 2). The lowest tested copper and nickel concentrations of 4  $\mu\text{g Cu/L}$  and 45  $\mu\text{g Ni/L}$  did not cause coral bleaching over 96 h and tentacles were commonly extended. After 36-h exposure, bleaching was observed in copper treatments of 11, 32 and 65  $\mu\text{g Cu/L}$  and the highest nickel treatment of 9050  $\mu\text{g Ni/L}$ . After 96-h exposure bleaching was observed in nickel treatments of 470 and 900  $\mu\text{g Ni/L}$ . Coral fragments from each treatment were given scores according to the Coral Watch health chart (Table S6).

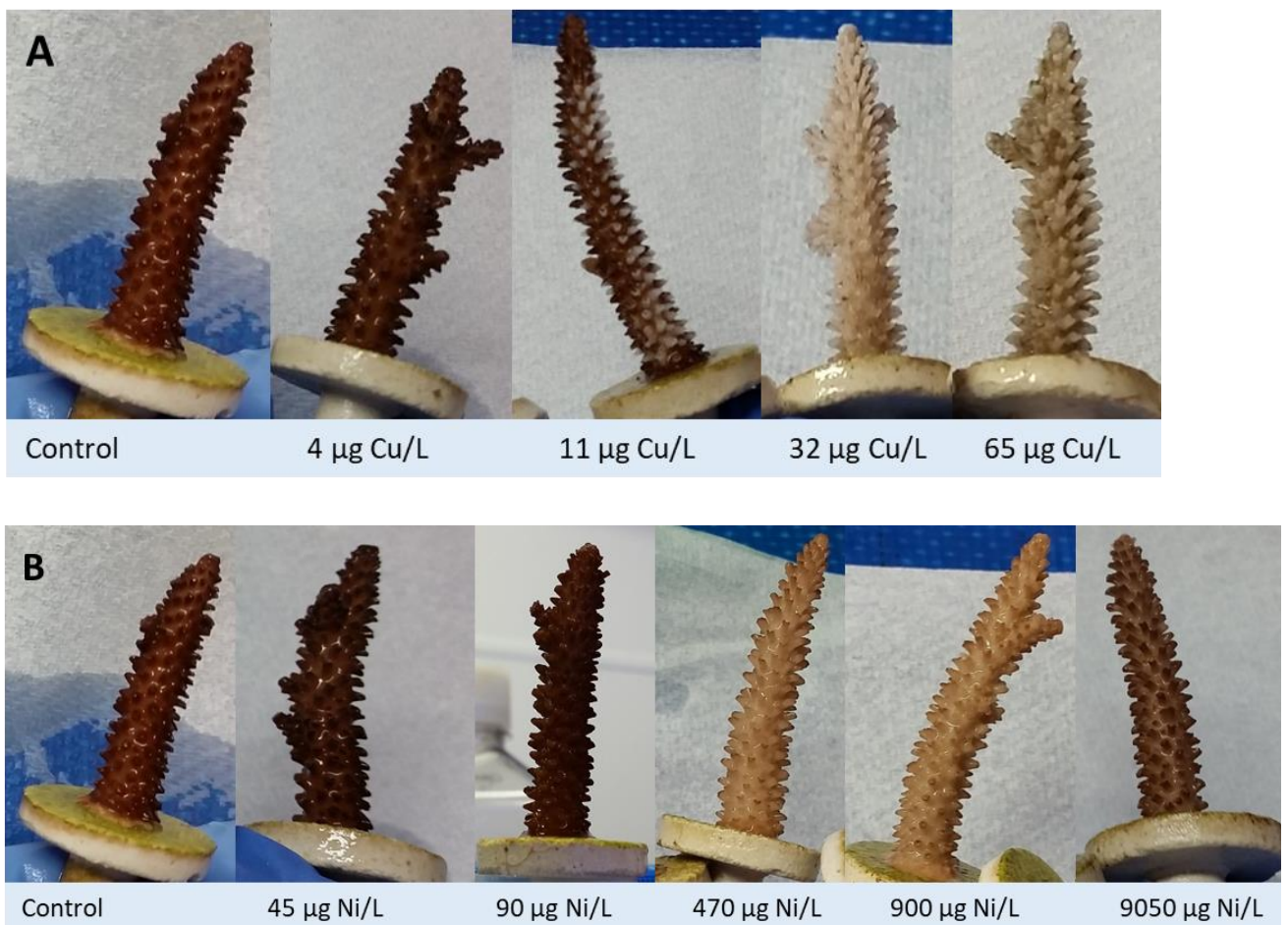


Figure 2. Photographs of the coral fragments following exposure to copper (A) and nickel (B) for 36-96 h. Corals exposed to 11, 32 and 65  $\mu\text{g Cu/L}$  and to 9050  $\mu\text{g Ni/L}$  were exposed for 36 h, all remaining treatment exposures ran for 96 h. Photos were taken as soon as corals were removed from the test chambers. Each photo is one representative replicate per treatment. Treatment concentrations are the measured, dissolved concentration (Table 4).

### 3.3. Metal uptake and distribution in corals

Concentrations of nickel and copper in coral tissues increased with increasing exposure concentration (Figure 3 A, B). The metal tissue concentration per surface area showed a similar trend (Supplementary Figure S1 A, B).

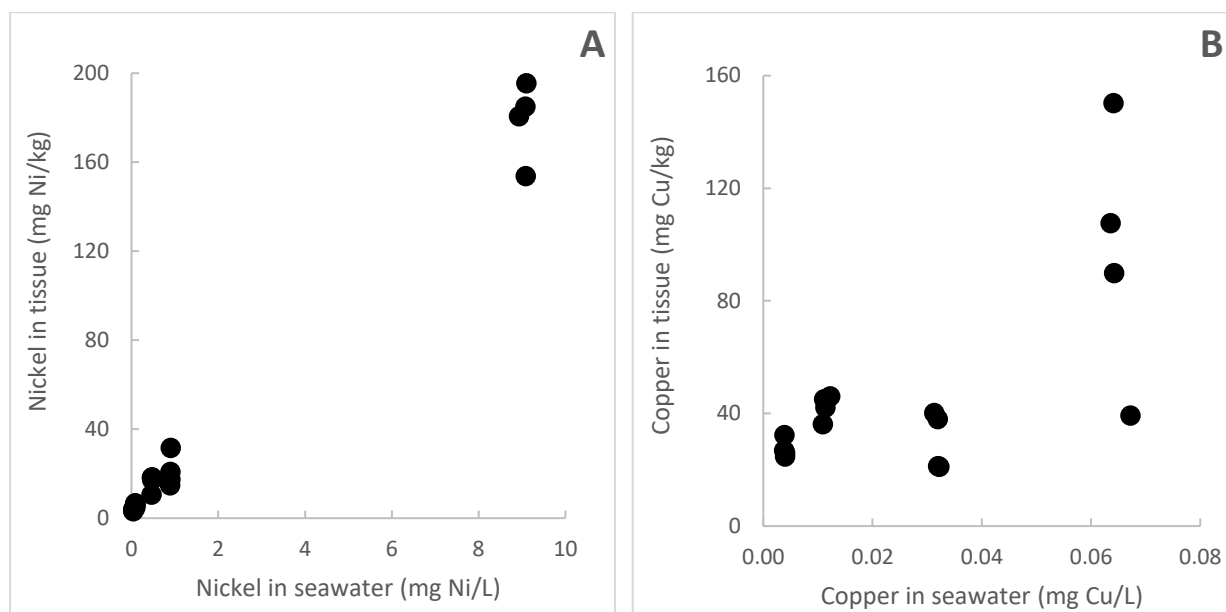


Figure 3. The effect of dissolved ( $0.45 \mu\text{m}$ ) metals in seawater on coral and *Symbiodinium* tissue concentrations for nickel (A) and copper (B). Each point represents one individual fragment from four replicate chambers per treatment. Note the different scales on the x-y axes.

### 3.4. Spatial distribution of nickel in coral fragments

Analysis by LA-ICPMS showed that nickel accumulated in a higher proportion in the proximal end (section B) than in the distal sections (C, D) of the coral fragment exposed to  $9050 \mu\text{g Ni/L}$  (Supplementary Figure S3). For section B of each treatment, there was a peak in nickel detected around the polyps of the coral fragments. We also found that the relative proportion of nickel in the coral fragments increased with increasing exposure concentration (Figure S4). This is correlated with a decrease in calcium detection, indicative of organic tissues. The LA-ICPMS data was in agreement with elemental maps generated from the  $\mu\text{-PIXE}$  which also detected peaks in nickel around the polyps, correlated with a decrease in calcium (Figures S5 and S6). The  $\mu\text{-PIXE}$  data also showed a peak in nickel within the axial polyp (Figure S5).

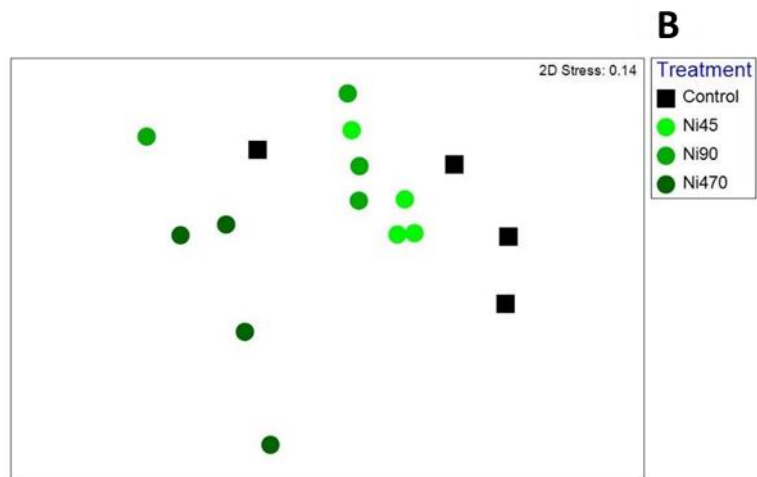
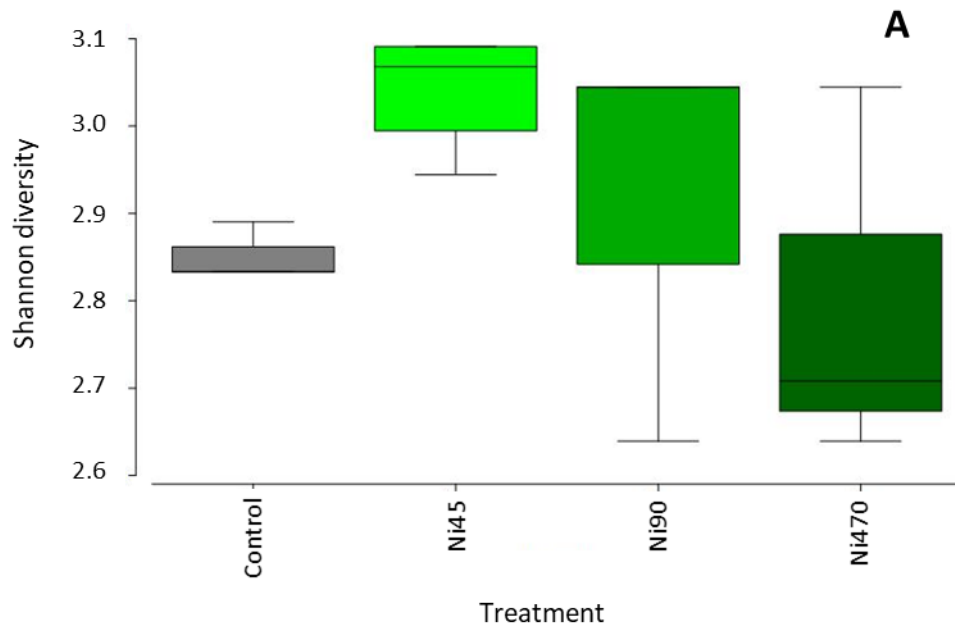
### 3.5. Community structure of the coral microbiome

All 18S data were transformed to presence/absence, therefore the analysis described below is referring to differences in richness of the OTUs associated with each taxonomic group. All 16S data were square root transformed, therefore analysis of 16S data refer to the relative abundances of the taxonomic groups across treatments. DNA extraction and amplification of coral tissues exposed to 900 and 9050  $\mu\text{g Ni/L}$  were unsuccessful, possibly due to insufficient tissue. Consequently, statistical analyses of the DNA metabarcoding results for nickel exposure were restricted to the control, 45, 90 and 470  $\mu\text{g Ni/L}$  treatments.

#### *Nickel - Eukaryotes*

Following 96-h exposure, the diversity in eukaryote (18S rDNA) taxa in the coral microbiome appeared to decline with increasing nickel concentration (Figure 4A); however, this was not statistically significant (ANOVA  $F = 1.06$ ,  $p = 0.22$ ). This may be due to the large variation in diversity observed at 90 and 470  $\mu\text{g Ni/L}$  and the relatively small sample size (Figure 4A). Figure 4B shows a statistically significant change in the composition of the eukaryotic community (PERMANOVA  $F = 2.9$ ,  $P = 0.01$ ), with the composition of the microbiomes from the highest nickel treatment (470  $\mu\text{g Ni/L}$ ) being different from the control and the lowest nickel treatment (45  $\mu\text{g Ni/L}$ ,  $P < 0.05$ ) (Figure 4B).

The major three taxa that contributed to the differences between the control and highest nickel treatment were OTUs associated with Chromadorea (26% contribution), Chlorophyceae (11%) and Bacillariophyceae (11%) (SIMPER analysis). When comparing the lowest nickel treatment (45  $\mu\text{g Ni/L}$ ) to the highest (470  $\mu\text{g Ni/L}$ ), the major three taxa that contributed to the differences were OTUs associated with Chromadorea (33%) and Phaeophyceae (10%). The shade plot in Figure 4C shows that as nickel exposures increased there was a decrease in the OTUs associated with Chromadorea and Phaeophyceae, and an increase in Chlorophyceae and Bacillariophyceae. Dinophyceae OTUs, which includes *Symbiodinium* remained unchanged across all treatments.



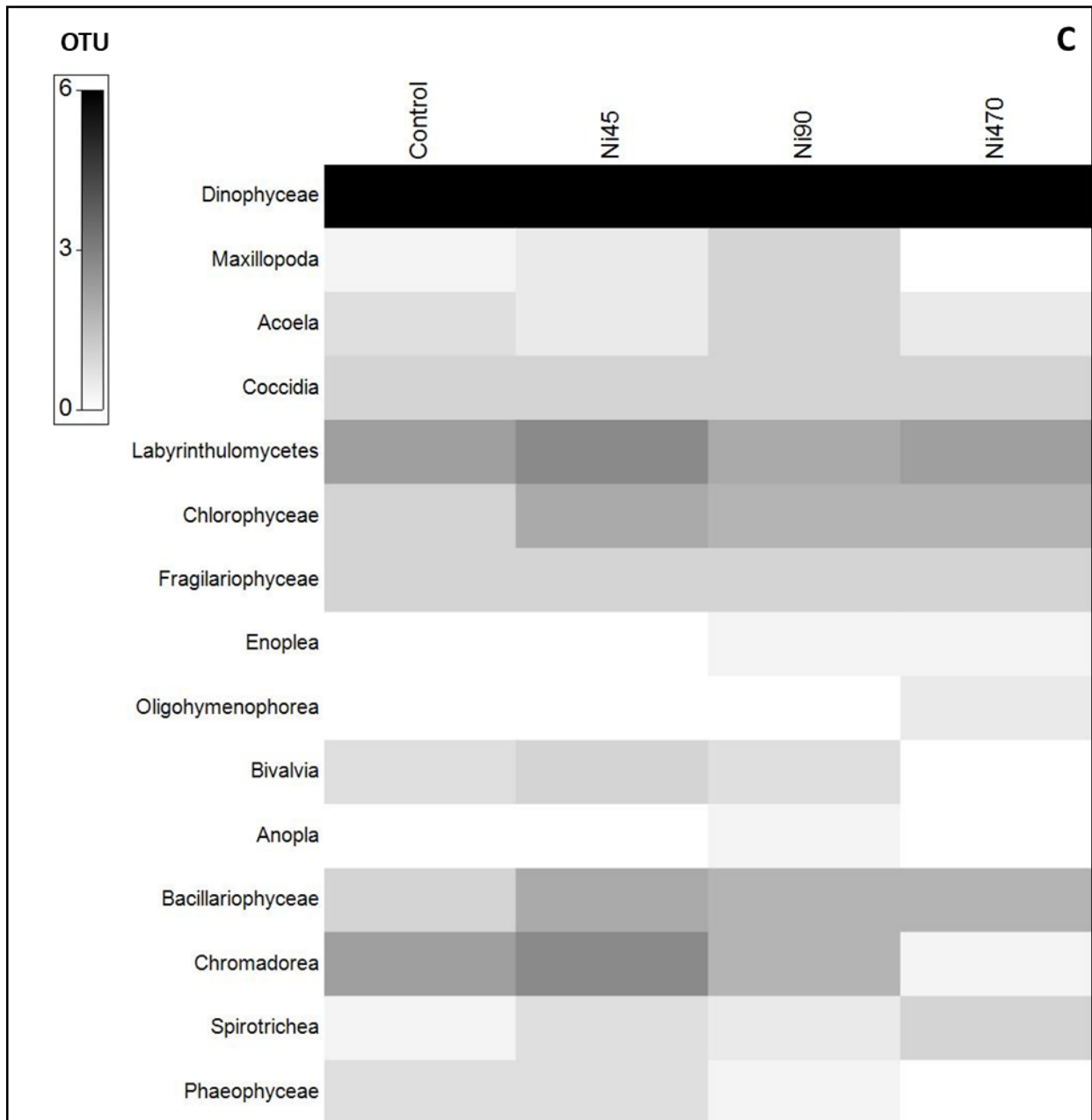


Figure 4. The effect of nickel on the eukaryote community composition of the coral microbiome following 96-h exposure to concentrations of 45, 90 and 470  $\mu\text{g Ni/L}$  (measured, dissolved, 0.45  $\mu\text{m}$ ) A) Boxplots showing the variation in Shannon diversity (median and interquartile range of 4 replicates) across control and nickel treatments B) Non-metric multidimensional scaling plot showing the relative similarity of the 18S community composition. Each point represents one individual replicate from each treatment. C) Shade plot demonstrating the changes in eukaryote taxa in response to increasing concentrations of nickel. Taxonomic level = class, OTU = Operational Taxonomic Units. Metal concentrations are measured dissolved values in  $\mu\text{g/L}$ .

## Nickel – Bacteria

Similar to the eukaryotic community, there was no significant difference in Shannon diversity between the control and nickel treatments in the bacterial community (ANOVA  $F = 0.94$ ,  $p = 0.45$ , Figure 5A). There was no significant difference in the bacterial community composition in relation to nickel treatment (PERMANOVA  $F = 1.7$ ,  $P = 0.11$ ), however there did appear to be a slight separation among the treatments (Figure 5B).

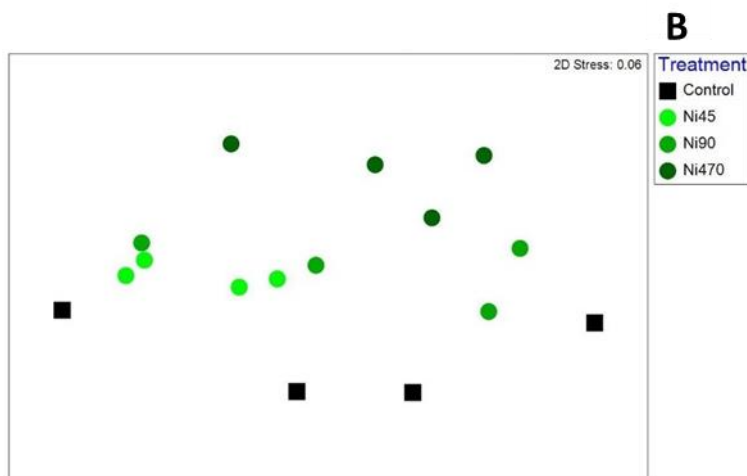
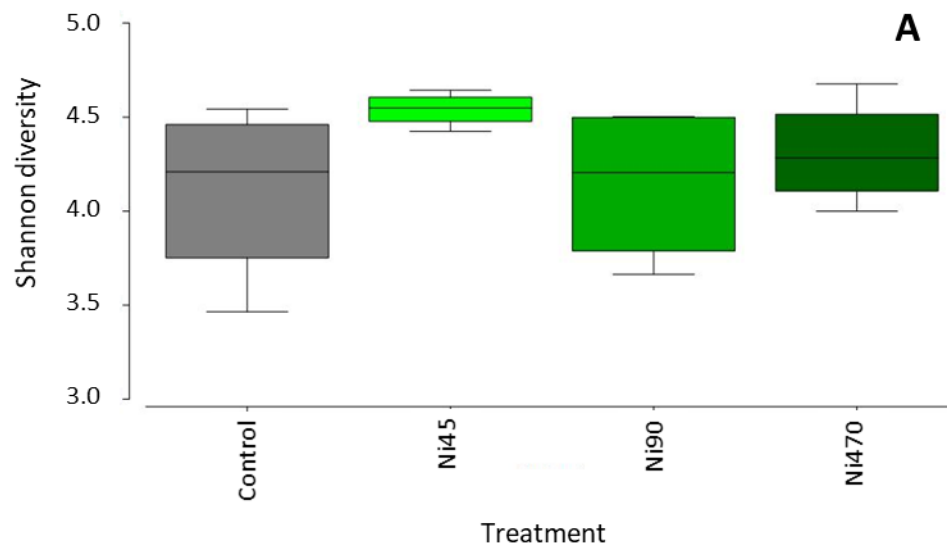


Figure 5. The effect of nickel on the bacterial community composition of the coral microbiome following 96-h exposure to concentrations of 45, 90 and 470  $\mu\text{g Ni/L}$  (measured, dissolved, 0.45  $\mu\text{m}$ ) A) Boxplots showing the variation in Shannon diversity (mean and interquartile range of 4 replicates) across control and nickel treatments. B) Non-metric multidimensional scaling plot showing the relative similarity of the 16S community composition. Each point represents one



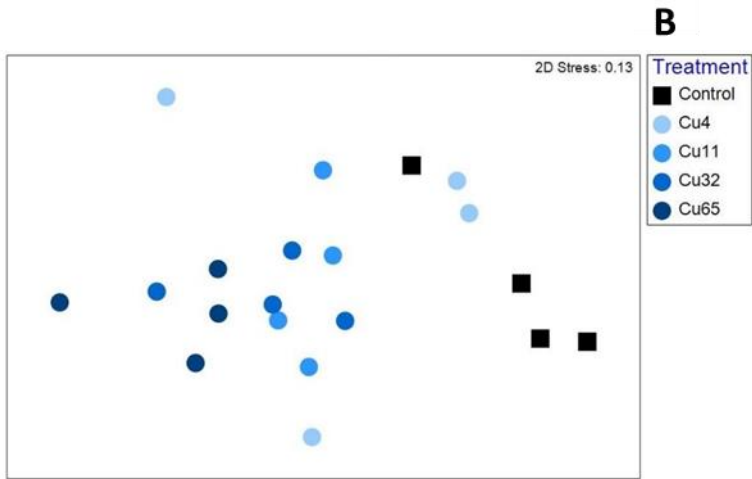
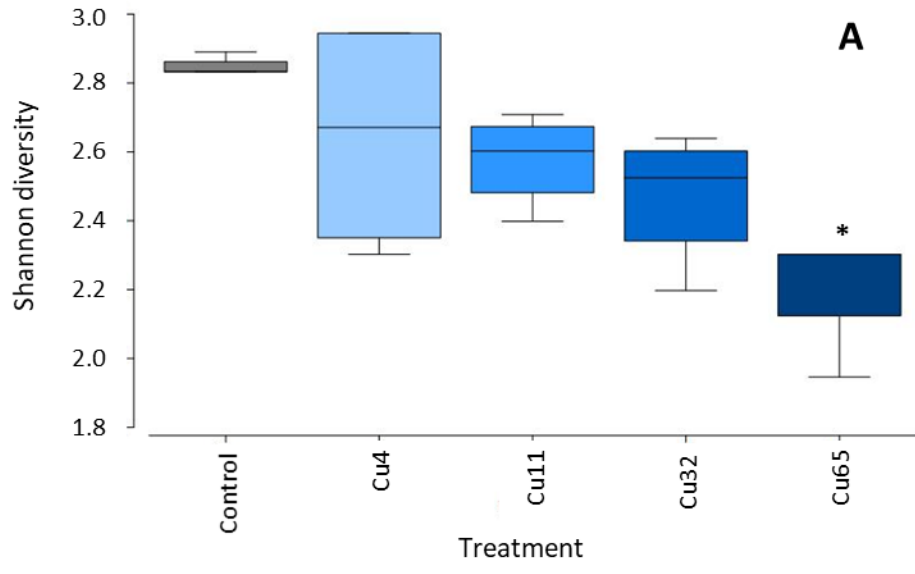
individual replicate from each treatment. Metal concentrations are measured dissolved values in  $\mu\text{g/L}$ .

### *Copper - Eukaryotes*

Following 36 – 96-h exposure to copper, there was a decrease in the eukaryote diversity of the coral microbiome with increasing copper concentration (Figure 6A), and the change in diversity across treatments was statistically significant (ANOVA  $F = 5.2$  and  $p = 0.007$ );  $65 \mu\text{g Cu/L}$  was significantly different to the control and  $4 \mu\text{g Cu/L}$  ( $p < 0.05$ ). It should be noted that corals were exposed to copper treatments of 11, 32 and  $65 \mu\text{g Cu/L}$  for 36 h, while control and  $4 \mu\text{g Cu/L}$  were exposed for 96 h.

Copper exposure was shown to alter the eukaryote community structure of the microbiomes of *A. muricata* (PERMANOVA  $F = 3.4$ ,  $P = 0.001$ ) (Figure 6B). The control and the lowest copper treatment ( $4 \mu\text{g Cu/L}$ ) had similar eukaryote communities ( $P > 0.05$ ), and the two highest copper treatments (32- $65 \mu\text{g Cu/L}$ ) were significantly different to the control, 4 and  $11 \mu\text{g Cu/L}$  treatments ( $P < 0.05$ ).

The taxa that were contributing to the differences between the control and the highest copper concentrations (11, 32,  $65 \mu\text{g/L}$ ) were OTUs associated with Chromadorea (23-29%), Labyrinthulomycetes (10-18%), Bacillariophyceae (10-11%) and Chlorophyceae (9-11%). As copper concentration increased there was a decrease in the OTUs associated with Chromadorea, Labyrinthulomycetes and Bacillariophyceae, with a subsequent increase in OTUs associated with Chlorophyceae (Figure 6C). The number of *Symbiodinium* OTUs, represented by Dinophyceae did not change across all treatments (Figure 6C).



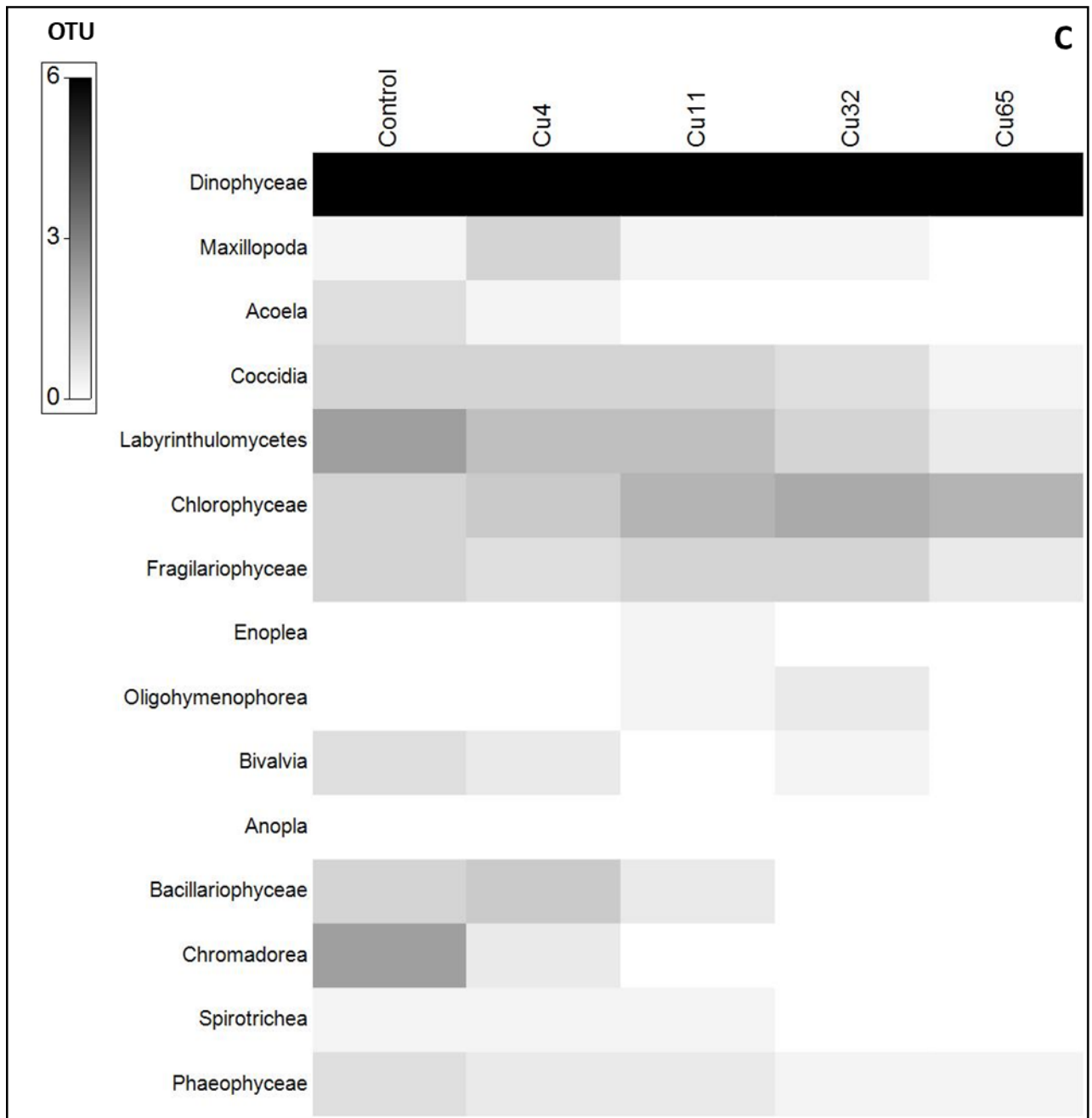


Figure 6. The effect of copper on the eukaryote community composition of the coral microbiome following 36 – 9 6-h exposure to concentrations of 4, 11, 32 and 65  $\mu\text{g Cu/L}$  (measured, dissolved, 0.45  $\mu\text{m}$ ) A) Boxplots showing the variation in Shannon diversity (mean and interquartile range of 4 replicates) across control and copper treatments, the asterisk indicates significant difference to the control. B) Non-metric multidimensional scaling plot showing the relative similarity of the 18S community composition. Each point represents one individual replicate from each treatment. C) Shade plot demonstrating the changes in the presence/absence of eukaryote taxa in response to increasing concentrations of copper.

Taxonomic level = Class, OTU = Operational Taxonomic Units. Metal concentrations are measured dissolved values in  $\mu\text{g/L}$ .

### *Copper – Bacteria*

While the data suggested that copper decreased bacterial diversity (Figure 7A), this was not found to be statistically significant ( $p > 0.05$ ). However, variation in diversity was markedly lower in the two highest treatments (Figure 7A).

Similar to the 18S rDNA data, the control and the lowest copper treatment (4  $\mu\text{g Cu/L}$ ) had a similar community composition (PERMANOVA  $F = 5.7$ ,  $P = 0.001$ , Figure 7B), and as copper concentration increased, the structure of the bacterial community changed significantly. The two highest copper treatments (32, 65  $\mu\text{g Cu/L}$ ) were significantly different to the control, 4 and 11  $\mu\text{g Cu/L}$  treatments (PERMANOVA  $P < 0.05$ ).

The significant differences between the copper treatments (11, 32, 65  $\mu\text{g/L}$ ) and the control were driven by Flavobacteriaceae (22-26%) Rhodobacteraceae (7-12%) Planctomycetaceae (8-9%) and Hahellaceae (8.2-15%). It appears that increasing copper concentration caused a decrease in Hahellaceae and Planctomycetaceae OTUs and a subsequent increase in OTUs associated with Flavobacteriaceae and Rhodobacteraceae (Figure 7C).

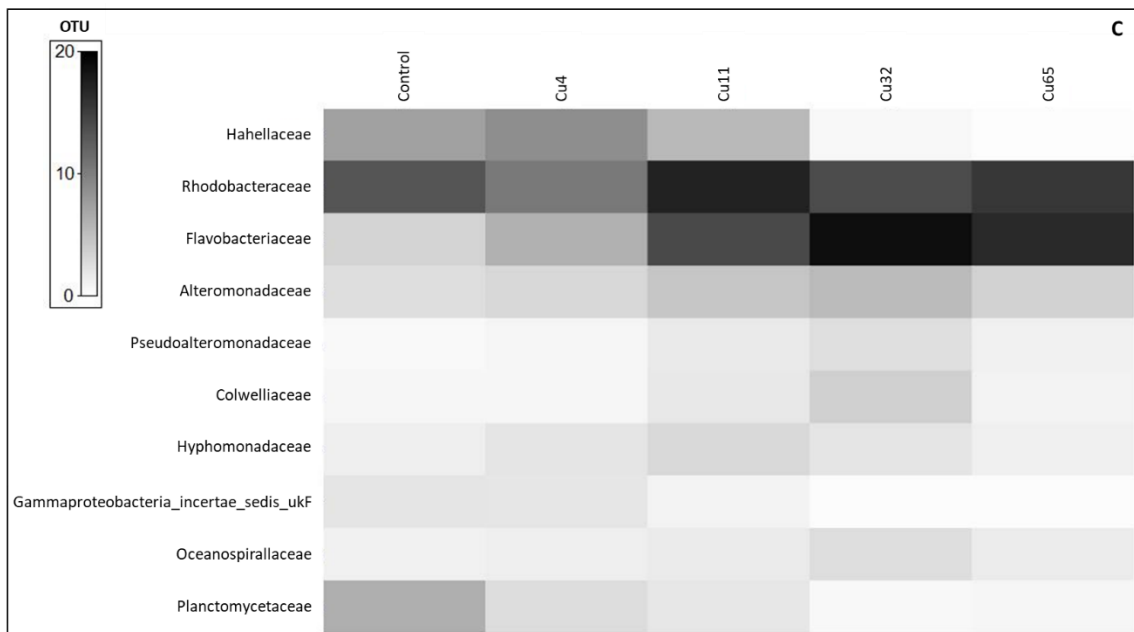
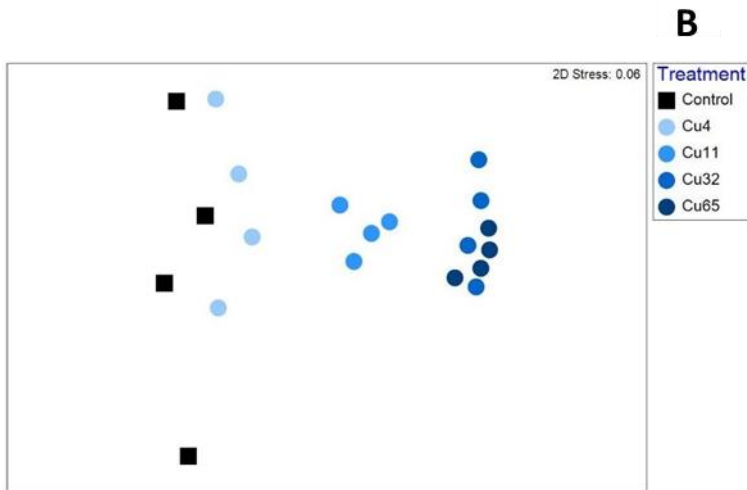
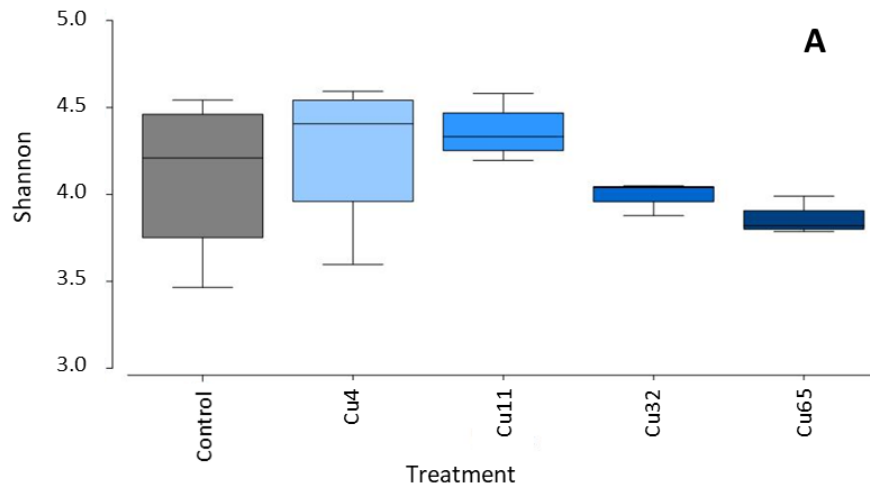


Figure 7. The effect of copper on the bacterial community composition of the coral microbiome following 36 to 96 -h exposure A) Boxplots showing the variation in Shannon diversity (mean and interquartile range of 4 replicates) across control and copper treatments. B) Non-metric multidimensional scaling plot showing the relative similarity of the 16S community composition. The (dis)similarity between control and copper treatments was determined by Bray-Curtis similarity. Each point represents one individual replicate from each treatment. C) Shade plot demonstrating the changes in taxa in response to increasing concentrations of nickel, note only the top 10 taxa are shown. Taxonomic level = Family, OTU = Operational Taxonomic Units, ukF= unknown Family, Family level not identified in classification. Metal concentrations are measured dissolved values in  $\mu\text{g/L}$ . Data were transformed by square root transformation.

#### **4. Discussion**

##### *4.1. Response of corals to nickel and copper exposure*

In this study bleaching was observed only at high nickel and copper concentrations ( $\geq 11 \mu\text{g Cu/L}$  and  $\geq 470 \mu\text{g Ni/L}$ ). These concentrations were tested to elucidate the full concentration response relationship, and would only be relevant for extremely polluted environments. Background concentrations of metals in tropical marine waters are typically  $< 1 \mu\text{g/L}$  for copper and  $< 5 \mu\text{g/L}$  for nickel (Apte et al., 2006), however in heavily polluted waters concentrations of dissolved nickel can exceed  $1000 \mu\text{g/L}$  (Pyle and Couture, 2012) and dissolved copper can exceed  $100 \mu\text{g/L}$  (Stauber et al., 2000). A study around New Caledonia, an area of prominent nickel mining activity measured nickel and copper concentrations ranging from  $< 0.1 - 11 \mu\text{g Ni/L}$  and  $< 0.1 - 1.6 \mu\text{g Cu/L}$  (Moreton et al., 2009).

At low concentrations metals, including copper and nickel are micronutrients, although there is limited evidence for nickel-deficiency or nickel-dependent biochemistry in aquatic biota (Blewett and Leonard, 2017; Chowdhury et al., 2008). Two studies from New Caledonia have demonstrated nickel and urea concentrations of  $< 3 \mu\text{g Ni/L}$  and  $< 6 \mu\text{mol/L}$ , respectively, enhance the calcification and growth of corals (Bisc  r   et al., 2018, 2017). In

combination with an additional stressor, elevated temperature (32°C), coral growth decreased (Biscéré et al., 2017).

Although we observed bleaching at high metal concentrations, coral tissues and polyps remained intact at the lowest copper concentration (11 µg Cu/L). Complete bleaching and polyp retraction was observed at the highest copper concentrations (32–65 µg Cu/L) (data not shown). We observed effects of copper on *A. muricata* at a lower concentration range compared to previous studies. Past studies which investigated the effects of other metals (copper, cadmium and lead) on the scleractinian coral, *Pocillopora damicornis*.

Mitchelmore et al. (2007) found that 50 µg/L of copper and cadmium (exposed individually for 14 days) did not cause bleaching but rather tissue sloughing in *P. damicornis*, where the entire coral tissue and *Symbiodinium* together separated from the skeleton eventually resulting in coral death (Mitchelmore et al., 2007). Hedouin et al. (2016) found that survival of adult *P. damicornis* decreased by 50% (LC50) between 175 - 250 µg Cu/L and 477 – 742 µg Pb/L, respectively.

The use of a colour scale to assess bleaching is a tool commonly used in the field to assess coral health (Coral Watch Chart 2014). To support this assessment, measurements of *Symbiodinium* density or photosynthesis activity could also be determined, and this has been explored in previous studies (Berry et al., 2016; Bessell-Browne et al., 2017; Biscéré et al., 2017). Metal bioaccumulation in corals was only a minor component of our study but this warrants further investigation in future.

#### 4.2. Metal uptake and distribution on corals

We found that with increasing high concentrations of nickel and copper in seawater, the metal concentrations in coral tissues (algal symbiont and host tissue) also increased. It is possible that the increased metal concentration measured in the coral tissues represents the loosely bound metal, or the fraction of metals adsorbed to the coral surface as opposed to absorbed internally, especially for those samples removed after a 36-h exposure, which were not rinsed with seawater.

Past studies have demonstrated that *Symbiodinium* play an important role in the accumulation and regulation of trace metals in cnidarian hosts (Hardefeldt and Reichelt-Brushett, 2015; Reichelt-Brushett and McOrist, 2003). *Symbiodinium* preferentially

accumulated zinc over the host, the anemone *Exaiptasia pallida*, after a 32-d chronic exposure (Hardefeldt and Reichelt-Brushett, 2015). The density of *Symbiodinium* plays an important role in controlling zinc loading in anemones (Hardefeldt and Reichelt-Brushett, 2015). An earlier study by Reichelt-Brushett and McOrist (2003) found that in corals sampled from the Great Barrier Reef (QLD, Australia), most metals (including nickel and copper) accumulated in higher concentrations in *Symbiodinium* than coral tissue. The authors concluded that the loss of *Symbiodinium* (i.e. bleaching) during stress events may play an important role in regulating metal loads in corals (Reichelt-Brushett and McOrist, 2003). Conversely, Mitchelmore et al. (2007) found no significant difference in the partitioning between the algal or animal fractions in the coral *P. damicornis* when exposed to copper or cadmium for 14 days. Hedouin et al., (2016) demonstrated, using radiotracer techniques, that nickel accumulated preferentially in the coral animal tissues and *Symbiodinium*, than in the skeleton of *Stylophora pistillata*, following a 14-d exposure. However, given that the overall contribution of nickel in *Symbiodinium* represented <7% of the whole nickel accumulation in corals, it was suggested that other biological processes controlled by the coral host were responsible for the accumulation of nickel in coral tissues (Hédouin et al., 2016). These studies highlight the importance of understanding the uptake and distribution of metals in host tissues and endosymbionts

#### 4.3. *Spatial distribution of nickel in coral fragments*

Past studies investigating metal accumulation in coral tissues utilised air blasting or water-pik to remove the tissue layer from the skeleton for acid digestion and analysis (Esslemont, 2000; Reichelt-Brushett and McOrist, 2003). Air blasting is an efficient means of tissue collection; however, the tissue associated with the internal section of the polyp may not be collected. Therefore, other techniques are required to measure metal accumulation inside the coral polyps. We trialled techniques including laser ablation ICP-MS (LA-ICP-MS) and  $\mu$ -PIXE to determine if nickel could be detected in the polyps of sectioned coral fragments. While quantitative data could not be obtained, elevated nickel concentrations were detected around the polyps in all coral fragments exposed to nickel. Additionally, as nickel exposure concentration increased, the nickel in the coral fragments also increased (Supplementary Figure S3). However, there is still a question around whether nickel is surface- adsorbed or absorbed (i.e. bioaccumulated) metal. To improve analysis of metal



accumulation with techniques such as LA-ICP-MS and  $\mu$ -PIXE more work is required to investigate rinsing techniques to remove loosely bound metal (e.g. EDTA rinses) and optimal preservation methods (particularly to keep tissues and skeletons intact). Traditionally, these techniques are used to analyse hard tissues, i.e. skeletons (Runnalls and Coleman, 2003), and further complications arise when attempting to incorporate analysis of both the hard and soft tissue components (Limbeck et al., 2015). We believe both techniques show promise for future analysis, particularly where there is interest in understanding the metal accumulation and distribution in coral polyps.

#### 4.4. *Changes in the coral microbiome*

Our findings clearly demonstrated that high concentrations of nickel and copper caused significant changes to eukaryote community structure of the microbiome of *A. muricata*. We observed a decline in metazoans for both nickel and copper, including Bivalvia and Chromadorea, as well as diatoms and brown algae including Bacillariophyceae (for copper only) and Phaeophyceae. The role of microalgae, other than dinoflagellates in coral microbiomes have yet to be elucidated, however it is possible, that diatoms and brown algae could also influence host-associated microbiomes by releasing carbon-containing photosynthates that fuel microbial metabolism (Bourne et al., 2013). Interestingly, for both copper and nickel, there was an increase in green algae, chlorophyceae. This possibly reflects the tolerance of chlorophyceae species to metal exposure, which has been demonstrated previously (Levy et al., 2007). Additionally, chlorophytes have been shown to increase in tropical sediments in response to anthropogenic inputs (Graham et al., in press). For both nickel and copper, there was no significant change in the OTUs associated with Dinophyceae which includes the algal endosymbiont, *Symbiodinium*. While bleaching was observed, indicating a loss in *Symbiodinium*, it was expected that this would be reflected in the metabarcoding data. However, the eukaryote data set was analysed based on presence/absence and not relative abundance. Future work should include *Symbiodinium* density counts, and *Symbiodinium* specific primers to investigate changes at a finer level of taxonomic resolution and abundance via the use of quantitative PCR.

The majority of coral microbiome studies have focused on changes on the bacterial or prokaryote component and less so on the eukaryotes, unless studying the algal endosymbiont, *Symbiodinium*. In a study on the effects of multiple stressors (tested

individually), increased temperature, reduced pH, elevated nutrients and dissolved organic carbon (DOC), Thurber et al. (2009) assessed changes in other eukaryote groups, as well as Alveolata (*Symbiodinium*), including Fungi, Metazoans, Rhodophyta (red algae) and Heterokontophyta (diatoms and brown algae). All stressors caused an increase, compared to control conditions, in Fungi, Metazoans, Rhodophyta and Heterokontophyta. It is not unexpected that primary producers such as Rhodophyta and Heterokontophyta would be stimulated by increased nutrients and carbon source. It is possible that an increase in Fungi was indicative of a disease-like state in the coral microbiome (Thurber et al., 2009b).

The relative abundance of bacteria and community composition of the coral microbiome were not affected by increasing nickel concentration. The overall community composition changed significantly with increasing copper and there was a decrease in relative abundance of Planctomycetaceae and Hahellaceae with a subsequent increase in Flavobacteriaceae and Rhodobacteriaceae. The increased presence of these bacterial taxa in *A. muricata* microbiome exposed to copper could indicate that the corals were stressed, potentially unable to regulate their microbiome and therefore became dominated by opportunistic and pathogenic taxa. Research into the bacterial genus *Endozoicomonas*, identified in this study under the family Hahellaceae, showed that they play a key role in the coral microbiome and participate in host-associated protein and carbohydrate transport and cycling (Neave et al., 2016). There was a significant decrease in Hahellaceae with increased copper exposure and this is a stress response consistently observed in other studies (McDevitt-Irwin et al., 2017). Studies have shown that reduced pH reduces abundance of *Endozoicomonas* in corals (Morrow et al., 2015; Webster et al., 2016). Ziegler et al. (2016) also observed a decrease in *Endozoicomonas* in coral microbiomes in response to sedimentation and sewage disposal in the Red Sea. The decline of *Endozoicomonas* in coral microbiomes in response to stress, as demonstrated here and in past studies, could be problematic for corals given the role this bacteria plays as a beneficial symbiont (McDevitt-Irwin et al., 2017; Neave et al., 2016).

Corals exposed to stressors may have a decreased ability to regulate their microbiome and so allowing the increased presence of potentially pathogenic and opportunistic microbial taxa (McDevitt-Irwin et al., 2017). In a literature review on the response of coral-associated bacteria to stressors including climate change, water pollution and overfishing, McDevitt et al., (2017) identified several taxa associated with stressed corals. These included

*Vibrionales*, *Flavobacteriales*, *Rhodobacteriales*, *Alteromonadales*, *Rhizobiales*, *Rhodospirillales* and *Desulfovibrionales*. Meron et al. (2011) found that reduced pH increased the presence of *Rhodobacteriales* in the coral microbiome of *Acropora eurystoma*. Gignoux-Wolfsohn and Vollmer (2015) found that corals with white-band disease (caused by bacterial pathogens) had a larger percentage of OTUs belonging to *Flavobacteriales*. In the coral *Pocillopora verrucosa*, *Flavobacteriales* was an indicator taxa for corals collected adjacent to municipal wastewater outfall areas (Ziegler et al., 2016).

#### 4.5. Results in context of overall health and function of corals

This study demonstrated that only exposures to highly elevated nickel and copper caused changes to the structure of the microbiome in the reef building coral *A. muricata*. The resulting imbalance in the microbiome could lead to functional changes and facilitate disease development or alterations in metabolism and immunity that lead to bleaching, necrosis and ultimately coral death (Glasl et al., 2017). While we observed structural changes in the coral microbiome there was a simultaneous increase in the tissue concentrations for both nickel and copper, and bleaching, albeit at the highest test concentrations. At lower concentrations, where bleaching was minimal or had not occurred, there were slight changes in the microbiome community structure. Increases in the number of treatment replicates could improve our ability to detect changes in the microbiome community structure, however this is a limitation of microcosm studies where large sample sizes are often not possible (Chariton et al., 2016; Ho et al., 2013). Another limitation to microcosm studies is that the experimental set up is essentially a closed system and the DNA of dead organisms could be attenuating our capacity to detect changes in the community. The use of RNA would reveal who in the community is living and functional (Chariton et al., 2014).

Given that micro-organisms respond rapidly to environmental conditions, it is vital to understand how the microbiome of corals responds to a range of natural and anthropogenic stressors. However, given the high concentrations used in this study, it is recommended that future work target lower, environmentally relevant concentrations to determine if the microbiome is altered in the same way. It is possible that the microbial community of corals could be used as an early warning indicator to identify stressed ecosystems prior to more

advanced visual cues such as tissue necrosis or bleaching, which are only evident when coral health has already become compromised (Glasl et al., 2017).

## 5. Conclusion

Coral reefs are subjected to numerous global and local stressors. In many tropical regions local stressors are likely to be associated with mining activities. To mitigate this risk requires an understanding of the potential impacts of metals on ecosystems. We used multiple lines of evidence to investigate the effects of copper and nickel, separately, on the common branching coral *Acropoa mucricata*. Following 36 – 96-h exposure we only observed bleaching at copper concentrations  $\geq 11 \mu\text{g Cu/L}$ , and nickel concentrations  $\geq 470 \mu\text{g Ni/L}$ . We found that as metal concentrations in the seawater increased, there was also an increase in copper and nickel concentrations in the coral tissues. We also observed significant changes to the microbiome community structure. Very high nickel concentrations of  $470 \mu\text{g Ni/L}$  altered the eukaryotic communities of the coral microbiome. For copper, significant differences in both the eukaryotic and bacterial communities were observed at  $\geq 11 \mu\text{g Cu/L}$ . Importantly, we detected a loss in Hahellaceae, a known beneficial bacteria in coral microbiomes, when exposed to copper. We also observed an increase in Flavobacteriaceae and Rhodobacteraceae two taxa which are believed to be indicative of stressed coral microbiomes. Collectively, our findings show that exposure to high concentrations of metals in polluted coastal waters, has the potential to alter the microbiome which is inherently linked to coral health via a range of symbiotic processes. Given the pivotal roles corals play in tropical ecosystems, considerably more research is required to determine how metals alter these coral holobionts, and to ensure that water quality guidelines are adequate for their protection, future studies are required to generate data for adult corals which can contribute to water quality guidelines development. In comparison to other marine invertebrates, corals are less sensitive to nickel and copper, however this not the case for other metals (e.g. (Summer et al., 2019). Future work should utilise lower test concentrations, investigate other physiological endpoints e.g. photosynthetic efficiency and *Symbiodinium* density and include field studies to investigate the effects of metal contaminants in the environment on corals and their microbiomes.

## **Acknowledgements**

Funding for this research was provided by NiPERA Inc., Proctor and Gamble Doctoral Fellowship in Environmental Science, Australian Institute of Nuclear Science and Engineering Scholarship, an Australian Government Research Training Program (RTP) Scholarship awarded to Francesca Gissi, and part funded by a grant from the Southern Cross University Marine Ecology Research Centre awarded to Amanda Reichelt-Brushett. We would like to thank the team at the National Sea Simulator (AIMS, Townsville, Australia), for collection and maintenance of corals, and assistance with setting up and running the experiment. We thank Keith Purnell, Dave Zahra, Henri Wong, Brett Rowling and Reiner Siegele (ANSTO) for preparation, analysis of corals at ANSTO and data interpretation, and Josh King and Chad Jarolimek (CSIRO) for assistance with metal analyses. We thank Graeme Batley, Merrin Adams and Sharon Hook (CSIRO) for reviewing the manuscript.

## References

- Andersson, A.F., Lindberg, M., Jakobsson, H., Bäckhed, F., Nyrén, P., Engstrand, L., 2008. Comparative analysis of human gut microbiota by barcoded pyrosequencing. *PLoS One* 3. <https://doi.org/10.1371/journal.pone.0002836>
- ANZECC/ARMCANZ, 2000. Australian and New Zealand Guidelines for Fresh and Marine Water Quality: National Water Quality Management Strategy Paper No.4. In Australian and New Zealand Environment and Conservation Council and Agriculture and Resource Management Council of Australia. Canberra, Australia.
- Aprill, A., McNally, S., Parsons, R., Weber, L., 2015. Minor revision to V4 region SSU rRNA 806R gene primer greatly increases detection of SAR11 bacterioplankton. *Aquat. Microb. Ecol.* 75, 129–137. <https://doi.org/10.3354/ame01753>
- Apte, S.C., Andersen, L.E., Andrewartha, J.R., Angel, B.M., Shrearer, D., Simpson, S.L., Stauber, J.L., Vicente-Beckett, V., 2006. Contaminant pathways in Port Curtis: Final Report. Technical Report 73. CRC for Coastal Zone, Estuary and Waterway Management.
- Baker, G.C., Smith, J.J., Cowan, D.A., 2003. Review and re-analysis of domain-specific 16S primers. *J. Microbiol. Methods* 55, 541–555. <https://doi.org/10.1016/j.mimet.2003.08.009>
- Berry, K.L.E., Hoogenboom, M.O., Flores, F., Negri, A.P., 2016. Simulated coal spill causes mortality and growth inhibition in tropical marine organisms. *Sci. Rep.* 6, 25894. <https://doi.org/10.1038/srep25894>
- Bessell-Browne, P., Negri, A.P., Fisher, R., Clode, P.L., Duckworth, A., Jones, R., 2017. Impacts of turbidity on corals: The relative importance of light limitation and suspended sediments. *Mar. Pollut. Bull.* 117, 161–170. <https://doi.org/10.1016/j.marpolbul.2017.01.050>
- Bielmyer, G.K., Grosell, M., Bhagooli, R., Baker, A.C., Langdon, C., Gillette, P., Capo, T.R., 2010. Differential effects of copper on three species of scleractinian corals and their algal symbionts (*Symbiodinium* spp.). *Aquat. Toxicol.* 97, 125–133. <https://doi.org/10.1016/j.aquatox.2009.12.021>
- Biscéré, T., Ferrier-Pagès, C., Grover, R., Gilbert, A., Rottier, C., Wright, A., Payri, C., Houlbrèque, F., 2018. Enhancement of coral calcification via the interplay of nickel and urease. *Aquat. Toxicol.* 200, 247–256. <https://doi.org/10.1016/j.aquatox.2018.05.013>
- Biscéré, T., Lorrain, A., Rodolfo-Metalpa, R., Gilbert, A., Wright, A., Devissi, C., Peignon, C., Farman, R., Duveilbourg, E., Payri, C., Houlbrèque, F., 2017. Nickel and ocean warming affect scleractinian coral growth. *Mar. Pollut. Bull.* 0–1. <https://doi.org/10.1016/j.marpolbul.2017.05.025>
- Biscere, T., Rodolfo-Metalpa, R., Lorrain, A., Chauvaud, L., Thebault, J., Clavier, J., Houlbrèque, F., 2015. Responses of two scleractinian corals to cobalt pollution and ocean acidification. *PLoS One* 10, 1–18. <https://doi.org/10.1371/journal.pone.0122898>
- Blewett, T.A., Leonard, E.M., 2017. Mechanisms of nickel toxicity to fish and invertebrates in

- marine and estuarine waters. *Environ. Pollut.* 223, 311–322.  
<https://doi.org/10.1016/j.envpol.2017.01.028>
- Bourne, D.G., Dennis, P.G., Uthicke, S., Soo, R.M., Tyson, G.W., Webster, N., 2013. Coral reef invertebrate microbiomes correlate with the presence of photosymbionts. *ISME J.* 7, 1452–1458. <https://doi.org/10.1038/ismej.2012.172>
- Chariton, A., Pettigrove, V., Baird, D., 2016. Ecological assessment, in: Simpson, S.L., Batley, G.E. (Eds.), *Sediment Quality Assessment: A Practical Guide*. CSIRO.
- Chariton, A.A., Ho, K.T., Proestou, D., Bik, H., Simpson, S.L., Portis, L.M., Cantwell, M.G., Baguley, J.G., Burgess, R.M., Pelletier, M.M., Perron, M., Gunsch, C., Matthews, R.A., 2014. A molecular-based approach for examining responses of eukaryotes in microcosms to contaminant-spiked estuarine sediments. *Environ. Toxicol. Chem.* 33, 359–369. <https://doi.org/10.1002/etc.2450>
- Chariton, A.A., Stephenson, S., Morgan, M.J., Steven, A.D.L., Colloff, M.J., Court, L.N., Hardy, C.M., 2015. Metabarcoding of benthic eukaryote communities predicts the ecological condition of estuaries. *Environ. Pollut.* 203, 165–174.  
<https://doi.org/10.1016/j.envpol.2015.03.047>
- Chowdhury, M.J., Bucking, C., Wood, C.M., 2008. Pre-exposure to waterborne nickel downregulates gastrointestinal nickel uptake in rainbow trout: Indirect evidence for nickel essentiality. *Environ. Sci. Technol.* 42, 1359–1364.  
<https://doi.org/10.1021/es071889n>
- Cole, J.R., Wang, Q., Fish, J.A., Chai, B., McGarrell, D.M., Sun, Y., Brown, C.T., Porrás-Alfaro, A., Kuske, C.R., Tiedje, J.M., 2014. Ribosomal Database Project: data and tools for high throughput rRNA analysis. *Nucleic Acids Res.* 42, D633–D642.  
<https://doi.org/10.1093/nar/gkt1244>
- Coral Watch, 2014. Coral Health Chart [WWW Document]. URL  
<https://www.coralwatch.org/web/guest/coral-health-chart> (accessed 6.21.18).
- Edgar, R.C., 2013. UPARSE: highly accurate OTU sequences from microbial amplicon reads. *Nat. Methods* 10, 996–998. <https://doi.org/10.1038/nmeth.2604>
- Egge, E., Bittner, L., Andersen, T., Audic, S., de Vargas, C., Edvardsen, B., 2013. 454 Pyrosequencing to Describe Microbial Eukaryotic Community Composition, Diversity and Relative Abundance: A Test for Marine Haptophytes. *PLoS One* 8.  
<https://doi.org/10.1371/journal.pone.0074371>
- Esslemont, G., 2000. Development and comparison of methods for measuring heavy metal concentrations in coral tissues. *Mar. Chem.* 69, 69–74. [https://doi.org/10.1016/S0304-4203\(99\)00096-1](https://doi.org/10.1016/S0304-4203(99)00096-1)
- Flores, F., Hoogenboom, M.O., Smith, L.D., Cooper, T.F., Abrego, D., Negri, A.P., 2012. Chronic exposure of corals to fine sediments: Lethal and sub-lethal impacts. *PLoS One* 7, 1–12. <https://doi.org/10.1371/journal.pone.0037795>
- Gignoux-Wolfsohn, S.A., Vollmer, S. V., 2015. Identification of Candidate Coral Pathogens on White Band Disease-Infected Staghorn Coral. *PLoS One* 10, e0134416.  
<https://doi.org/10.1371/journal.pone.0134416>

- Gissi, F., Stauber, J., Reichelt-Brushett, A., Harrison, P.L., Jolley, D.F., 2017. Inhibition in fertilisation of coral gametes following exposure to nickel and copper. *Ecotoxicol. Environ. Saf.* 145. <https://doi.org/10.1016/j.ecoenv.2017.07.009>
- Gissi, F., Stauber, J.L., Binet, M.T., Golding, L.A., Adams, M.S., Schlekot, C.E., Garman, E.R., Jolley, D.F., 2016. A review of nickel toxicity to marine and estuarine tropical biota with particular reference to the South East Asian and Melanesian region. *Environ. Pollut.* 218, 1308–1323. <https://doi.org/10.1016/j.envpol.2016.08.089>
- Gissi, F., Stauber, J.L., Binet, M.T., Trenfield, M.A., Van Dam, J.W., Jolley, D.F., 2018. Assessing the chronic toxicity of nickel to a tropical marine gastropod and two crustaceans. *Ecotoxicol. Environ. Saf.* 159. <https://doi.org/10.1016/j.ecoenv.2018.05.010>
- Glasl, B., Webster, N.S., Bourne, D.G., 2017. Microbial indicators as a diagnostic tool for assessing water quality and climate stress in coral reef ecosystems. *Mar. Biol.* 164, 1–18. <https://doi.org/10.1007/s00227-017-3097-x>
- Goh, B.P.L., 1991. Mortality and Settlement Success of *Pocillopora damicornis* Planula Larvae during Recovery from Low Levels of Nickel. *Pacific Sci.* 45, 276–286.
- Graham, S.E., Chariton, A.A., Landis, W.G., n.d. Using Bayesian networks to Predict Risk to Estuary Water Quality and Patterns of Benthic Environmental DNA in Queensland. *Integr. Environ. Assess. Manag.*
- Grottoli, A.G., Martins, P.D., Wilkins, M.J., Johnston, M.D., Warner, M.E., Cai, W.J., Melman, T.F., Hoadley, K.D., Pettay, D.T., Levas, S., Schoepf, V., 2018. Coral physiology and microbiome dynamics under combined warming and ocean acidification. *PLoS One* 13. <https://doi.org/10.1371/journal.pone.0191156>
- Hardefeldt, J.M., Reichelt-Brushett, A.J., 2015. Unravelling the role of zooxanthellae in the uptake and depuration of an essential metal in *Exaiptasia pallida*; an experiment using a model cnidarian. *Mar. Pollut. Bull.* 96, 294–303. <https://doi.org/10.1016/j.marpolbul.2015.04.055>
- Hardy, C.M., Krull, E.S., Hartley, D.M., Oliver, R.L., 2010. Carbon source accounting for fish using combined DNA and stable isotope analyses in a regulated lowland river weir pool. *Mol. Ecol.* 19, 197–212. <https://doi.org/10.1111/j.1365-294X.2009.04411.x>
- Hédouin, L., Metian, M., Teyssié, J.L., Oberhänsli, F., Ferrier-Pagés, C., Warnau, M., 2016. Bioaccumulation of <sup>63</sup>Ni in the scleractinian coral *Stylophora pistillata* and isolated Symbiodinium using radiotracer techniques. *Chemosphere* 156, 420–427. <https://doi.org/10.1016/j.chemosphere.2016.04.097>
- Hedouin, L.S., Wolf, R.E., Phillips, J., Gates, R.D., 2016. Improving the ecological relevance of toxicity tests on scleractinian corals: Influence of season, life stage, and seawater temperature. *Environ. Pollut.* 213, 240–253. <https://doi.org/10.1016/j.envpol.2016.01.086>
- Hernandez-Agreda, A., Gates, R.D., Ainsworth, T.D., 2017. Defining the Core Microbiome in Corals' Microbial Soup. *Trends Microbiol.* 25, 125–140. <https://doi.org/10.1016/j.tim.2016.11.003>



- Ho, K.T., Chariton, A.A., Portis, L.M., Proestou, D., Cantwell, M.G., Baguley, J.G., Burgess, R.M., Simpson, S., Pelletier, M.C., Perron, M.M., Gunsch, C.K., Bik, H.M., Katz, D., Kamikawa, A., 2013. Use of a novel sediment exposure to determine the effects of triclosan on estuarine benthic communities. *Environ. Toxicol. Chem.* 32, 384–392. <https://doi.org/10.1002/etc.2067>
- Jones, R.J., 1997. Zooxanthellae loss as a bioassay for assessing stress in corals. *Mar. Ecol. Prog. Ser.* 149, 163–171. <https://doi.org/10.3354/meps149163>
- Levy, J.L., Stauber, J.L., Jolley, D.F., 2007. Sensitivity of marine microalgae to copper: The effect of biotic factors on copper adsorption and toxicity. *Sci. Total Environ.* 387, 141–154. <https://doi.org/10.1016/J.SCITOTENV.2007.07.016>
- Limbeck, A., Galler, P., Bonta, M., Bauer, G., Nischkauer, W., Vanhaecke, F., 2015. Recent advances in quantitative LA-ICP-MS analysis: Challenges and solutions in the life sciences and environmental chemistry ABC Highlights: Authored by Rising Stars and Top Experts. *Anal. Bioanal. Chem.* 407, 6593–6617. <https://doi.org/10.1007/s00216-015-8858-0>
- McDevitt-Irwin, J.M., Baum, J.K., Garren, M., Vega Thurber, R.L., 2017. Responses of Coral-Associated Bacterial Communities to Local and Global Stressors. *Front. Mar. Sci.* 4. <https://doi.org/10.3389/fmars.2017.00262>
- Meron, D., Atias, E., Iasur Kruh, L., Elifantz, H., Minz, D., Fine, M., Banin, E., 2011. The impact of reduced pH on the microbial community of the coral *Acropora eurystoma*. *ISME J.* 5, 51–60. <https://doi.org/10.1038/ismej.2010.102>
- Mitchellmore, C.L., Verde, E.A., Weis, V.M., 2007. Uptake and partitioning of copper and cadmium in the coral *Pocillopora damicornis*. *Aquat. Toxicol.* 85, 48–56. <https://doi.org/10.1016/j.aquatox.2007.07.015>
- Moreton, B.M., Fernandez, J.-M., Dolbecq, M.B.D., 2009. Development of a Field Preconcentration/Elution Unit for Routine Determination of Dissolved Metal Concentrations by ICP-OES in Marine Waters: Application for Monitoring of the New Caledonia Lagoon. *Geostand. Geoanalytical Res.* 33, 205–218. <https://doi.org/10.1111/j.1751-908X.2009.00899.x>
- Morrow, K.M., Bourne, D.G., Humphrey, C., Botté, E.S., Laffy, P., Zaneveld, J., Uthicke, S., Fabricius, K.E., Webster, N.S., 2015. Natural volcanic CO<sub>2</sub> seeps reveal future trajectories for host-microbial associations in corals and sponges. *ISME J.* 9. <https://doi.org/10.1038/ismej.2014.188>
- Neave, M.J., Apprill, A., Ferrier-Pagès, C., Voolstra, C.R., 2016. Diversity and function of prevalent symbiotic marine bacteria in the genus *Endozoicomonas*. *Appl. Microbiol. Biotechnol.* <https://doi.org/10.1007/s00253-016-7777-0>
- Negri, A.P., Flores, F., Röthig, T., Uthicke, S., 2011. Herbicides increase the vulnerability of corals to rising sea surface temperature. *Limnol. Oceanogr.* 56, 471–485. <https://doi.org/10.4319/lo.2011.56.2.0471>
- Negri, A.P., Heyward, A.J., 2001. Inhibition of coral fertilisation and larval metamorphosis by tributyltin and copper. *Mar. Environ. Res.* 51, 17–27. [39](https://doi.org/10.1016/S0141-</a></p>
</div>
<div data-bbox=)

- Nystrom, M., Nordemar, I., Tedengren, M., 2001. Simultaneous and sequential stress from increased temperature and copper on the metabolism of the hermatypic coral *Porites cylindrica*. *Mar. Biol.* 138, 1225–1231. <https://doi.org/10.1007/s002270100549>
- Paulino, G.V.B., Broetto, L., Pylro, V.S., Landell, M.F., 2016. Compositional shifts in bacterial communities associated with the coral *Palythoa caribaeorum* due to anthropogenic effects. *Mar. Pollut. Bull.* 114, 1024–1030. <https://doi.org/10.1016/j.marpolbul.2016.11.039>
- Peixoto, R., Rosado, P., Leite, D., Rosado, A.S., Bourne, D., 2017. Beneficial Microorganisms for Corals (BMC): proposed mechanisms for coral health and resilience. *Front. Microbiol.* 8, 1–16. <https://doi.org/10.3389/fmicb.2017.00341>
- Pyle, G. and Couture, P., 2012. Nickel, in: C.M. Wood, A.P. Farrell, C.J.B. (Ed.), *Homeostasis and Toxicology of Non-Essential Metals*. Academic Press, London, UK, pp. 254–292.
- Quast, C., Pruesse, E., Yilmaz, P., Gerken, J., Schweer, T., Yarza, P., Peplies, J., Glöckner, F.O., 2012. The SILVA ribosomal RNA gene database project: improved data processing and web-based tools. *Nucleic Acids Res.* 41, D590–D596. <https://doi.org/10.1093/nar/gks1219>
- Quince, C., Lanzen, A., Davenport, R.J., Turnbaugh, P.J., 2011. Removing noise from pyrosequenced amplicons. *BMC Bioinformatics* 12, 38.
- Reichelt-Brushett, A., Hudspith, M., 2016. The effects of metals of emerging concern on the fertilization success of gametes of the tropical scleractinian coral *Platygyra daedalea*. *Chemosphere* 150, 398–406. <https://doi.org/10.1016/j.chemosphere.2016.02.048>
- Reichelt-Brushett, A.J., Harrison, P.L., 2005. The effect of selected trace metals on the fertilization success of several scleractinian coral species. *Coral Reefs* 24, 524–534. <https://doi.org/10.1007/s00338-005-0013-5>
- Reichelt-Brushett, A.J., Harrison, P.L., 2000. The effect of copper on the settlement success of larvae from the scleractinian coral *Acropora tenuis*. *Mar. Pollut. Bull.* 41, 385–391. [https://doi.org/10.1016/S0025-326X\(00\)00131-4](https://doi.org/10.1016/S0025-326X(00)00131-4)
- Reichelt-Brushett, A.J., McOrist, G., 2003. Trace metals in the living and nonliving components of scleractinian corals. *Mar. Pollut. Bull.* 46, 1573–1582. [https://doi.org/10.1016/S0025-326X\(03\)00323-0](https://doi.org/10.1016/S0025-326X(03)00323-0)
- Rothig, T., Ochsenkuhn, M.A., Roik, A., Van Der Merwe, R., Voolstra, C.R., 2016. Long-term salinity tolerance is accompanied by major restructuring of the coral bacterial microbiome. *Mol. Ecol.* 25, 1308–1323. <https://doi.org/10.1111/mec.13567>
- Runnalls, L.A., Coleman, M.L., 2003. Record of natural and anthropogenic changes in reef environments (Barbados West Indies) using laser ablation ICP-MS and sclerochronology on coral cores. *Coral Reefs* 22, 416–426. <https://doi.org/10.1007/s00338-003-0349-7>
- Ryan, C.G., 2001. Developments in Dynamic Analysis for quantitative PIXE true elemental imaging. *Nucl. Instruments Methods Phys. Res. Sect. B Beam Interact. with Mater. Atoms* 181, 170–179. [https://doi.org/10.1016/S0168-583X\(01\)00374-3](https://doi.org/10.1016/S0168-583X(01)00374-3)

- Ryan, C.G., Jamieson, D.N., Churms, C.L., Pilcher, J.V., 1995. A new method for on-line true-elemental imaging using PIXE and the proton microprobe. *Nucl. Instruments Methods Phys. Res. Sect. B Beam Interact. with Mater. Atoms* 104, 157–165. [https://doi.org/10.1016/0168-583X\(95\)00404-1](https://doi.org/10.1016/0168-583X(95)00404-1)
- Siegele, R., Cohen, D.D., Dytlewski, N., 1999. The ANSTO high energy heavy ion microprobe. *Nucl. Instruments Methods Phys. Res. Sect. B Beam Interact. with Mater. Atoms* 158, 31–38. [https://doi.org/10.1016/S0168-583X\(99\)00393-6](https://doi.org/10.1016/S0168-583X(99)00393-6)
- Stauber, J.L., Benning, R.J., Hales, L.T., Eriksen, R., Nowak, B., 2000. Copper bioavailability and amelioration of toxicity in Macquarie Harbour, Tasmania, Australia. *Mar. Freshw. Res.* 51, 1–10. <https://doi.org/10.1071/MF99010>
- Summer, K., Reichelt-Brushett, A., Howe, P., 2019. Toxicity of manganese to various life stages of selected marine cnidarian species. *Ecotoxicol. Environ. Saf.* 167, 83–94. <https://doi.org/10.1016/j.ecoenv.2018.09.116>
- Thurber, R.V., Willner-Hall, D., Rodriguez-Mueller, B., Desnues, C., Edwards, R.A., Angly, F., Dinsdale, E., Kelly, L., Rohwer, F., 2009a. Metagenomic analysis of stressed coral holobionts. *Environ. Microbiol.* 11, 2148–2163. <https://doi.org/10.1111/j.1462-2920.2009.01935.x>
- Thurber, R.V., Willner-Hall, D., Rodriguez-Mueller, B., Desnues, C., Edwards, R.A., Angly, F., Dinsdale, E., Kelly, L., Rohwer, F., 2009b. Metagenomic analysis of stressed coral holobionts. *Environ. Microbiol.* 11, 2148–2163. <https://doi.org/10.1111/j.1462-2920.2009.01935.x>
- USEPA, 2005. National Recommended Water Quality Criteria. United States Environmental Protection Agency, Office of Water [WWW Document]. URL <http://www.epa.gov/waterscience/criteria/wqctable/> (accessed 4.1.17).
- USGS, 2016. U. S. Geological Survey, Mineral Commodities Summaries January 2016. Nickel. [WWW Document]. URL <https://minerals.usgs.gov/minerals/pubs/commodity/nickel/mcs-2016-nicke.pdf> (accessed 2.27.18).
- Webster, N.S., Negri, A.P., Botté, E.S., Laffy, P.W., Flores, F., Noonan, S., Schmidt, C., Uthicke, S., 2016. Host-associated coral reef microbes respond to the cumulative pressures of ocean warming and ocean acidification. *Nat. Publ. Gr.* 1–9. <https://doi.org/10.1038/srep19324>
- Webster, N.S., Negri, A.P., Botté, E.S., Laffy, P.W., Flores, F., Noonan, S., Schmidt, C., Uthicke, S., 2016. Host-associated coral reef microbes respond to the cumulative pressures of ocean warming and ocean acidification. *Sci. Rep.* 6, 19324. <https://doi.org/10.1038/srep19324>
- Webster, N.S., Webb, R.I., Ridd, M.J., Hill, R.T., Negri, A.P., 2001. The effects of copper on the microbial community of a coral reef sponge. *Environ. Microbiol.* 3, 19–31. <https://doi.org/10.1046/j.1462-2920.2001.00155.x>
- Zhang, Y.Y., Ling, J., Yang, Q.S., Wang, Y.S., Sun, C.C., Sun, H.Y., Feng, J. Bin, Jiang, Y.F.,

Zhang, Y.Z., Wu, M.L., Dong, J. De, 2015. The diversity of coral associated bacteria and the environmental factors affect their community variation. *Ecotoxicology* 24, 1467–1477. <https://doi.org/10.1007/s10646-015-1454-4>

Ziegler, M., Roik, A., Porter, A., Zubier, K., Mudarris, M.S., Ormond, R., Voolstra, C.R., 2016. Coral microbial community dynamics in response to anthropogenic impacts near a major city in the central Red Sea. *Mar. Pollut. Bull.* 105, 629–640. <https://doi.org/10.1016/j.marpolbul.2015.12.045>

## Supplementary material

**Table S1.** PCR conditions for amplification of DNA using various primers

Primer set	PCR conditions		
	Denature (°C, mins)	Annealing (°C, secs)	Extension (°C, mins)
18S	95, 2	40 cycles: 95, 30 58, 30 72, 60	72, 7
16S	94, 3	35 cycles: 94, 45 50, 60 72, 90	72, 10

**Table S2.** Total number of reads and operational taxonomic units (OTUs) prior to and after filtering the data in preparation for statistical analysis.

Dataset	Before filtering		After filtering	
	OTUs	Reads	OTUs	Reads
18S rDNA	681	3290956	30	2387661
16S rDNA	2163	1859154	209	1443382

**Table S3.** Background concentrations of metals in filtered seawater used to make treatment solutions each day during the 4 day exposure. LOD = Limit of detection. Values in bold exceeded the LOD.

	Al	As	Ba	Be	Cd	Co	Cr	Cu	Fe	Fe	Mn	Ni	Pb	Se	Zn
LOD	0.52	0.76	0.05	0.003	0.56	0.24	1.1	0.31	0.60	3.9	0.21	1.8	1.9	3.0	0.12
T=0	<b>1.3</b>	<0.76	<b>0.51</b>	<0.003	<0.56	<0.24	<1.1	<b>1.3</b>	<b>3.6</b>	<3.9	<0.21	<1.8	<1.9	<3.0	<0.12
T=1	<b>1.0</b>	<0.76	<b>0.61</b>	<0.003	<0.56	<0.24	<1.1	<0.31	<b>4.3</b>	<b>4.1</b>	<0.21	<1.8	<1.9	<3.0	<0.12
T=2	<b>2.6</b>	<0.76	<b>0.54</b>	<0.003	<0.56	<0.24	<1.1	<b>2.1</b>	<0.60	<3.9	<0.21	<1.8	<1.9	<3.0	<b>2.0</b>
T=3	<b>0.5</b>	<0.76	<b>0.17</b>	<0.003	<0.56	<0.24	<1.1	<0.31	<0.60	<3.9	<0.21	<1.8	<b>2.1</b>	<3.0	<0.12

**Table S4.** Concentrations of dissolved and total nickel and copper, measured in the treatment tanks on days 0-3. Sub-samples were taken immediately after treatment solutions were made. NM = not measured. These treatments were sacrificed at 36 h and so treatment solutions were not made on days 2-3.

Treatment	Day			
	0	1	2	3
Dissolved (<0.45 $\mu\text{m}$ ), $\mu\text{g/L}$				
Control	0.0	0.0	0.8	0.3
Ni50	47	47	45	45
Ni100	92	92	93	93
Ni500	493	474	467	457
Ni1000	914	910	912	902
Ni10000	9167	9066	NM	NM
Control	1.3	1.0	2.1	0.4
Cu5	5.6	4.6	4.7	4.6
Cu20	17	17	NM	NM
Cu50	46	43	NM	NM
Cu100	89	85	NM	NM
Total, $\mu\text{g/L}$				
Control	0.0	0.2	0.6	0.6
Ni50	48	47	49	46
Ni100	96	92	94	92
Ni500	513	485	479	468
Ni1000	939	924	921	914
Ni10000	9601	9387	NM	NM
Control	1.2	0.9	1.4	0.6
Cu5	4.6	5.8	4.7	4.8
Cu20	19	27	NM	NM
Cu50	48	46	NM	NM
Cu100	88	89	NM	NM

**Table S5.** Concentrations of total nickel and copper, measured in the test chambers on Day 0 and day 1 or 4.

Treatment	Day			
	0		1 or 4	
	Mean <sup>a</sup>	SD <sup>a</sup>	Mean <sup>a</sup>	SD <sup>a</sup>
Total, µg/L				
Control	0.0	0.7	0.4	0.7
Ni50	43	0.6	46	0.3
Ni100	87	0.4	91	0.8
Ni500	483	6.9	464	5.1
Ni1000	894	11	912	3.3
Ni10000 <sup>b</sup>	8955	85	9216	75
Control	3.2	0.5	0.8	0.0
Cu5	4.1	0.3	3.2	0.2
Cu20 <sup>b</sup>	13	0.5	12	0.9
Cu50 <sup>b</sup>	35	0.9	40	1.5
Cu100 <sup>b</sup>	69	2.0	70	1.6

<sup>a</sup> Taken from 4 replicate chambers

<sup>b</sup> These treatments were sacrificed and samples taken for analysis on day 1 (not on day 4), due to bleaching.

**Table S6.** Coral watch health chart scores for coral fragments following exposure to nickel and copper for 36-96 h. (<https://www.coralwatch.org/web/guest/coral-health-chart>)

Treatment	Score	Description
Control	D5-D6	Healthy branching coral
4 µg Cu/L	D5-D6	Healthy branching coral
11 µg Cu/L	D3	Slightly bleached
32 µg Cu/L	D1	Severely bleached
65 µg Cu/L	D2	Moderately bleached
45 µg Ni/L	D5-D6	Healthy branching coral
90 µg Ni/L	D1	Severely bleached
470 µg Ni/L	D2	Moderately bleached
900 µg Ni/L	D2	Moderately bleached
9050 µg Ni/L	D2	Moderately bleached



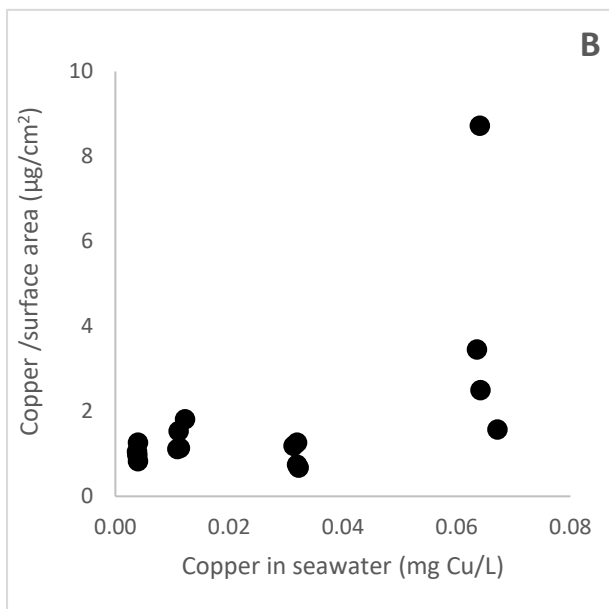
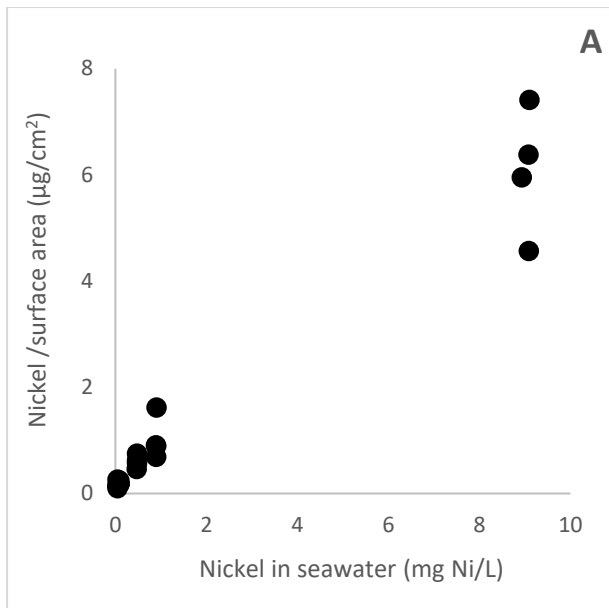
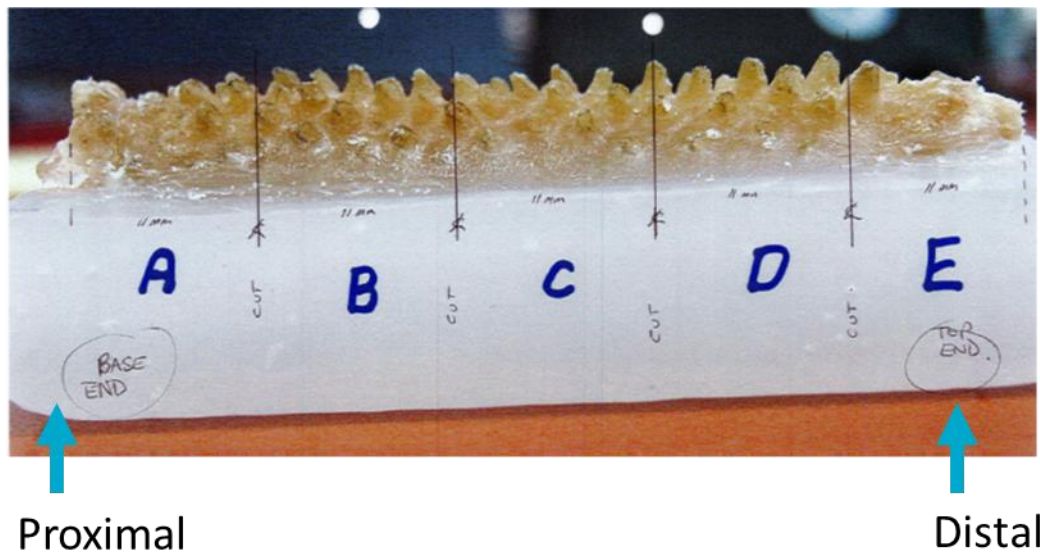
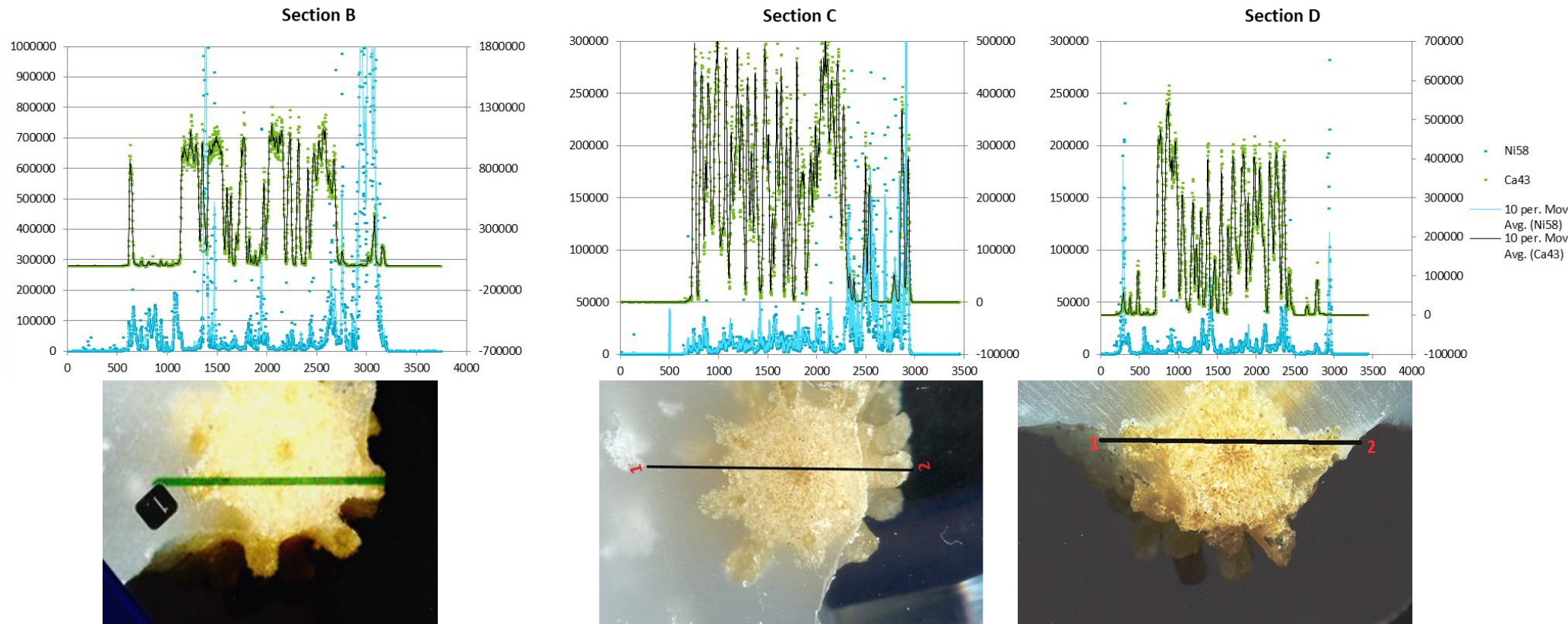


Figure S1. The concentration of nickel (A) and copper (B) per surface area of the coral fragment, versus measured dissolved (0.45-µm) metal concentration in the test chambers. Each point represents one individual fragment from four replicate chambers per treatment. Note the different scales on the x-y axes.

**Figure S2.** Photograph to demonstrate how the coral fragments were embedded in paraffin wax and cut into sections using a diamond blade cutter prior to analysis with LA-ICPMS.



**Figure S3.** Analysis of a coral fragment exposed to 9050  $\mu\text{g Ni/L}$  (measured, dissolved) by laser-ablation ICP-MS. Data shows the relative proportion of nickel and calcium detected along the laser line, marked out in the photographs. Measurements on x-axis indicate the location of the laser across the coral section; measurements on the y-axis indicate the number of counts for calcium (left-hand axis) and nickel (right hand axis). Each point is averaged across six data points.



**Figure S4.** Analysis of a coral fragments exposed to seawater (control), 90, 900 and 9050  $\mu\text{g Ni/L}$  (measured, dissolved) by laser-ablation ICP-MS. Only section B of each fragment was analysed. Data shows the relative proportion of nickel and calcium detected along the laser line, marked out in the photographs. Measurements on x-axis indicate the location of the laser across the coral section; measurements on the y-axis indicate the number of counts for calcium (left-hand axis) and nickel (right hand axis). Each point is averaged across six data points.

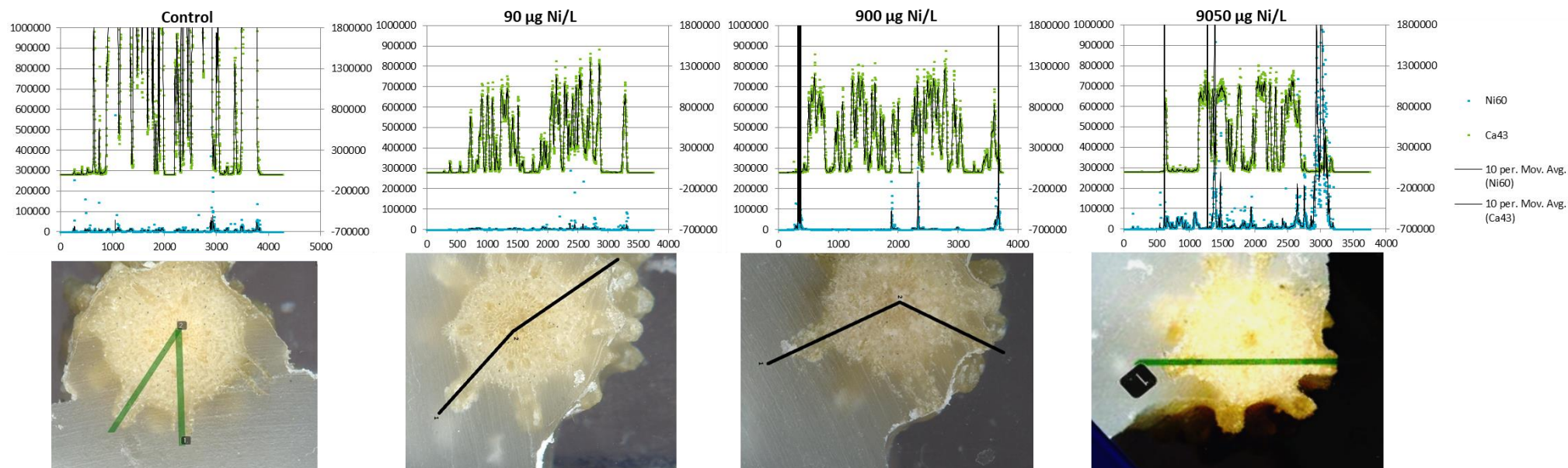


**Figure S5** Maps from  $\mu$ -PIXE analysis showing the detection of calcium (A) and nickel (B) of the section B (Figure S1) taken from a coral fragment exposed to 9050  $\mu\text{g Ni/L}$  (measured dissolved). The scale bar indicates the relative level of element detected in the sample in the top image. The blue rectangles in the bottom image mark the path of analysis. Figure A provides an example of the location and image of the external or radial polyps, the central or axial polyp and the porous coral skeleton.

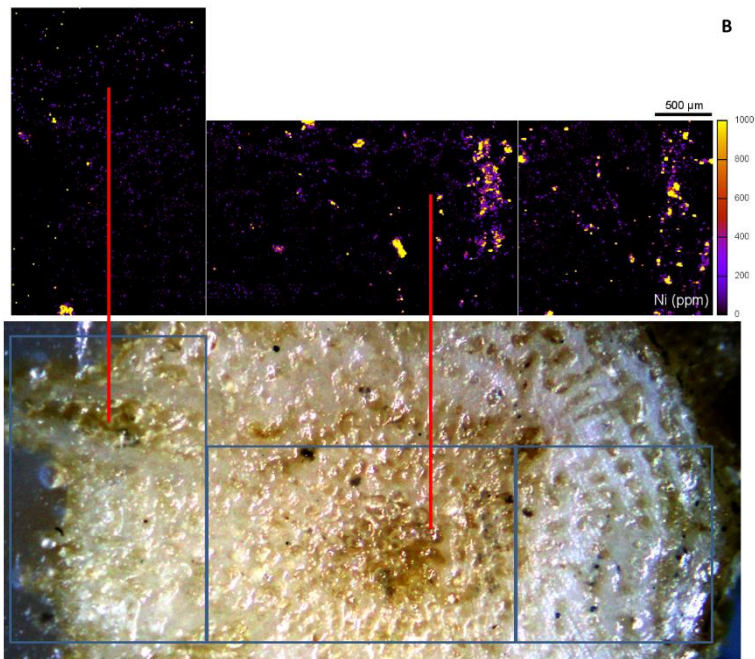
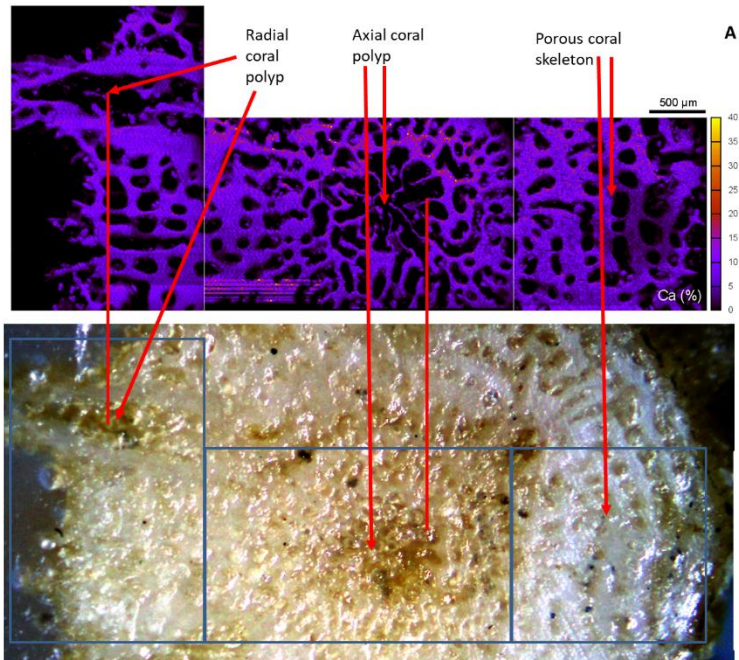
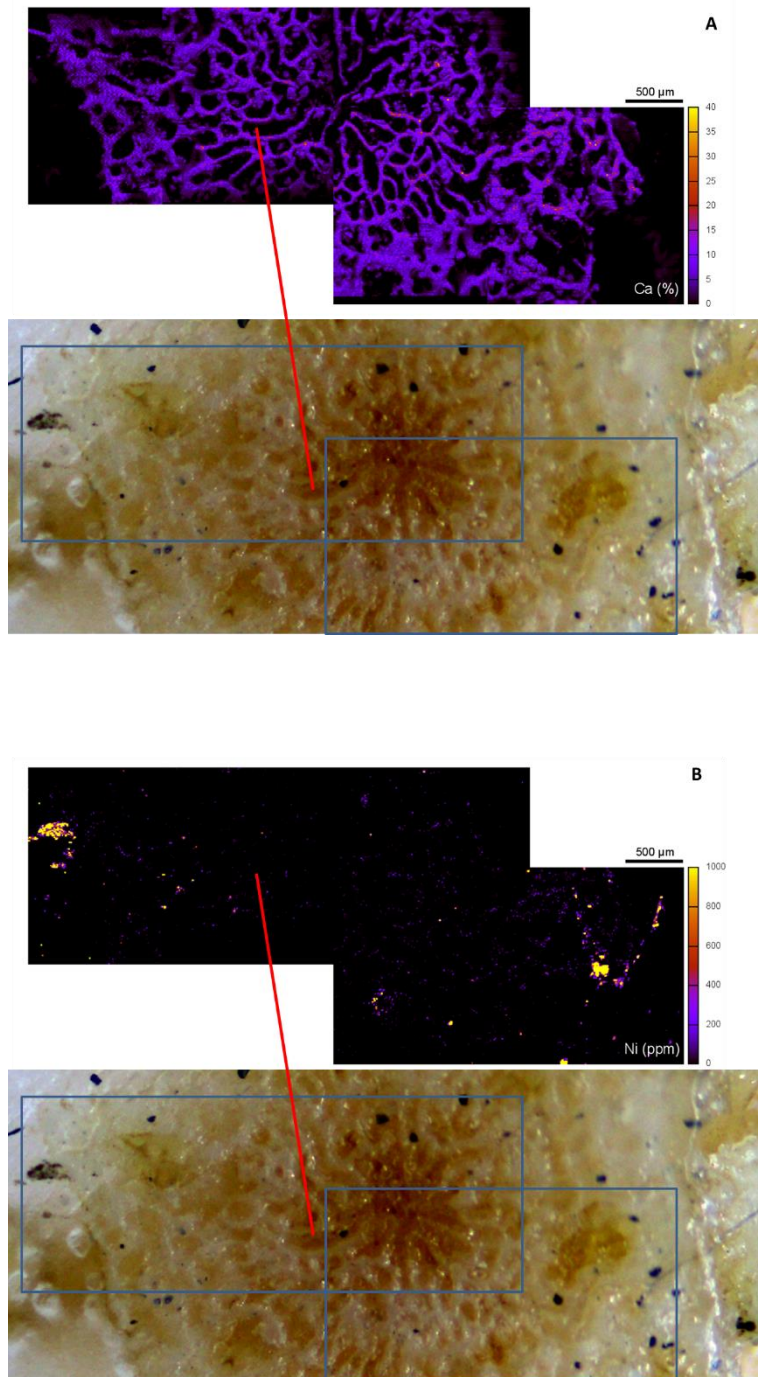


**Figure S6** Maps from  $\mu$ -PIXE analysis showing the detection of calcium (A) and nickel (B) of the section D (Figure S1) taken from a coral fragment exposed to 9050  $\mu\text{g Ni/L}$  (measured dissolved). The scale bar indicates the relative level of element detected in the sample in the top image. The blue rectangles in the bottom image mark the path of analysis.



## DNA amplification and sequencing using 16S\_V5-V6 region primers

Primers: 784f (5'-3': AGGATTAGATACCCTGGTA), 1061r (5'-3': CRRACGAGCTGACGAC) for the V5 and V6 region of the 16S rRNA gene (Andersson et al., 2008; Ziegler et al., 2016).

Polymerase Chain Reaction (PCR) methods are described in the paper. All amplifications used the Amplitaq Gold 360 Master Mix (MM, Applied Biosystems), and DNA-free water (brand). For 16S\_V5-6 primers the total PCR reaction volume was 50µL which consisted of 25µL of MM, 1µL of each primer, 20µL of water and 3 µL of template DNA.

PCR conditions:

	PCR conditions		
	Denature	Annealing	Extension
16S_V5-6	95°C 15 mins	35 cycles: 95°C 20 secs, 55°C 90 secs, 72°C 60 secs	72°C 7 mins

Total number of reads and operational taxonomic units (OTUs) prior to and after filtering the data in preparation for statistical analysis.

	Before filtering		After filtering	
Dataset	OTUs	Reads	OTUs	Reads
16S_V5-6	1606	1347465	207	1158830

Sequence data was processed through the bioinformatics pipeline and filtered, as per methods in main paper. Statistical analysis followed methods described for 16S in main paper.

### *Bacteria – 16S\_V5-6*

The general trends observed in the 16S\_V4 dataset were similar to the trends in the community structure amplified with the 16S\_V5-6 primer set. The bacterial community structure in all nickel treatments were not significantly different to the control. However the highest and lowest nickel treatments were found to be significantly different ( $p < 0.05$ , Figure 13A). The three highest copper treatments were significantly different to the control and the lowest copper treatment (Figure 13B,  $p < 0.05$ ).

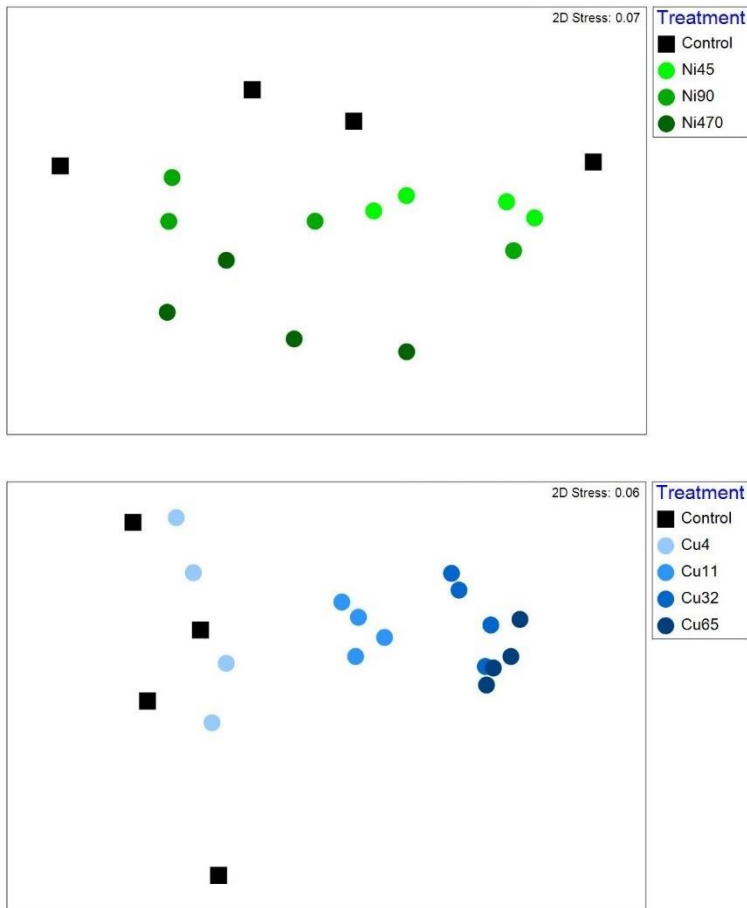


Figure S7. Non-metric multidimensional scaling plots for the 16S\_V5-6 dataset for nickel (A) and copper (B). The (dis)similarity between treatments was determined by Bray-Curtis similarity, data were standardised and then square-root transformed. Each point represents one individual replicate from each treatment.

In this dataset, the significant drivers of the differences between the lowest and highest nickel treatment were Rhodobacteraceae (26%) and Hahellaceae (11%). In the copper treatments the main taxa that were driving the differences between the high copper concentrations and the control and lowest copper were Flavobacteriaceae (21-26%) and Hahellaceae (13-20%) and Rhodobacteraceae (14-17%). Similar to the 16S\_V4 dataset, the shade plots in Figure 14 show that there appears to be a slight decrease in the number of Rhodobacteraceae OTUs with increasing nickel concentration. Hahellaceae decreases with increasing copper concentration as Flavobacteriaceae and Rhodobacteraceae OTUs increase (Figure 14). While Planctomycetaceae was detected by the 16S\_V5-6 primers, it was not indicated as a key driver of the differences between the bacterial communities in the copper or nickel treatments, unlike the 16S\_V4 primers.